



HAL
open science

Modelling dynamic soil organic carbon flows of annual and perennial energy crops to inform energy-transport policy scenarios in France

Ariane Albers, Angel Avadi, Anthony Benoist, Pierre Collet, Arnaud Hélias

► **To cite this version:**

Ariane Albers, Angel Avadi, Anthony Benoist, Pierre Collet, Arnaud Hélias. Modelling dynamic soil organic carbon flows of annual and perennial energy crops to inform energy-transport policy scenarios in France. *Science of the Total Environment*, 2020, 718, pp.135278. 10.1016/j.scitotenv.2019.135278 . hal-02566462

HAL Id: hal-02566462

<https://hal.inrae.fr/hal-02566462>

Submitted on 7 May 2020

HAL is a multi-disciplinary open access archive for the deposit and dissemination of scientific research documents, whether they are published or not. The documents may come from teaching and research institutions in France or abroad, or from public or private research centers.

L'archive ouverte pluridisciplinaire **HAL**, est destinée au dépôt et à la diffusion de documents scientifiques de niveau recherche, publiés ou non, émanant des établissements d'enseignement et de recherche français ou étrangers, des laboratoires publics ou privés.

1
2
3
4
5
6
7
8
9
10
11
12
13
14
15
16
17
18
19
20
21
22
23
24
25
26
27
28
29
30
31
32
33
34
35
36
37
38
39
40
41
42
43
44
45
46
47
48
49
50
51
52
53
54
55
56
57
58
59
60
61
62
63
64
65

Modelling dynamic soil organic carbon flows of annual and perennial energy crops to inform energy-transport policy scenarios in France

Ariane Albers^{a, b, c, *}, Angel Avadí^{c, d, f}, Anthony Benoist^{c, e, f}, Pierre Collet^a, Arnaud Hélias^{b, g, h}

^a IFP Energies Nouvelles, 1 et 4 Avenue de Bois-Préau, 92852 Rueil-Malmaison, France

^b LBE, Montpellier SupAgro, INRA, UNIV Montpellier, Narbonne, France

^c Elsa, Research Group for Environmental Lifecycle and Sustainability Assessment, Montpellier, France

^d CIRAD, UPR Recyclage et risque, F-34398 Montpellier, France

^e CIRAD, UPR BioWooEB, F-34398 Montpellier, France

^f Univ Montpellier, CIRAD, Montpellier, France

^g Chair of Sustainable Engineering, Technische Universität Berlin, Berlin, Germany

^h ITAP, Irstea, Montpellier SupAgro, Univ Montpellier, ELSA Research Group, Montpellier, France

* Corresponding author: ariane.albers@ifpen.fr

Modelling dynamic soil organic carbon flows of annual and perennial energy crops to inform energy-transport policy scenarios in France

Ariane Albers^{a, b, c, *}, Angel Avadí^{c, d, f}, Anthony Benoist^{c, e, f}, Pierre Collet^a, Arnaud Hélias^{b, g, h}

^a IFP Energies Nouvelles, 1 et 4 Avenue de Bois-Préau, 92852 Rueil-Malmaison, France

^b LBE, Montpellier SupAgro, INRA, UNIV Montpellier, Narbonne, France

^c Elsa, Research Group for Environmental Lifecycle and Sustainability Assessment, Montpellier, France

^d CIRAD, UPR Recyclage et risque, F-34398 Montpellier, France

^e CIRAD, UPR BioWooEB, F-34398 Montpellier, France

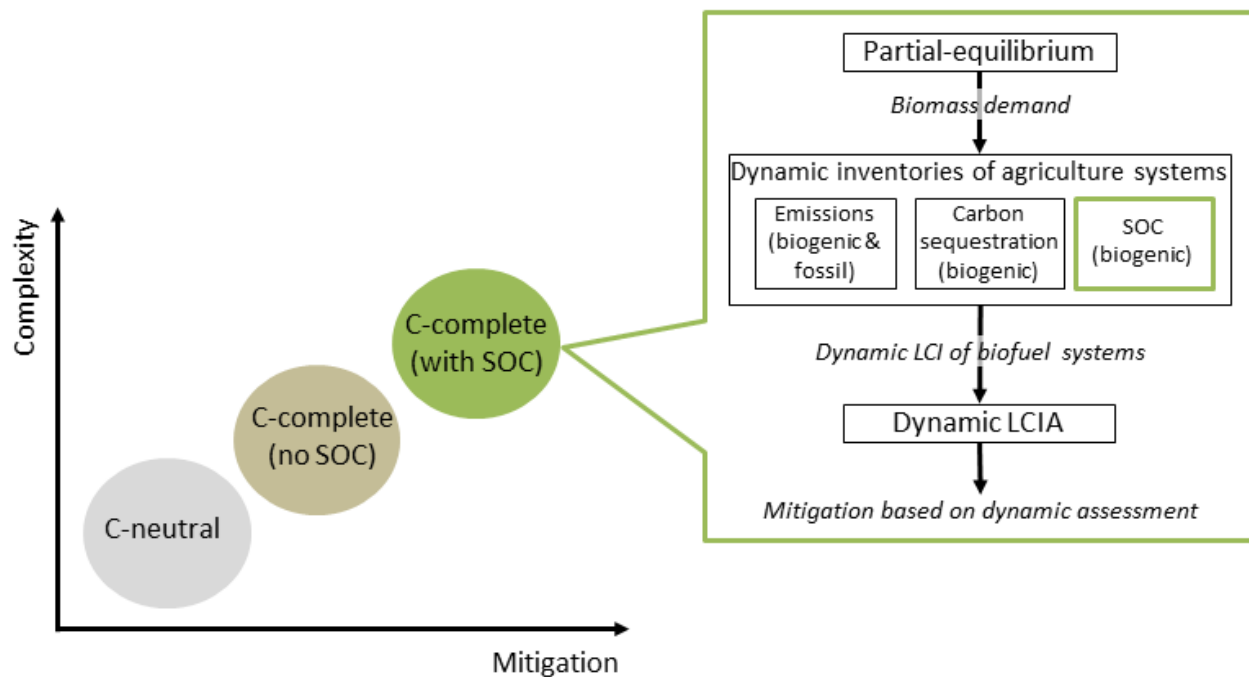
^f Univ Montpellier, CIRAD, Montpellier, France

^g Chair of Sustainable Engineering, Technische Universität Berlin, Berlin, Germany

^h ITAP, Irstea, Montpellier SupAgro, Univ Montpellier, ELSA Research Group, Montpellier, France

* Corresponding author: ariane.albers@ifpen.fr

Graphical abstract



Modelling dynamic soil organic carbon flows of annual and perennial energy crops to inform energy-transport policy scenarios in France

Ariane Albers^{a, b, c, *}, Angel Avadí^{c, d, f}, Anthony Benoist^{c, e, f}, Pierre Collet^a, Arnaud Hélias^{b, g, h}

^a IFP Energies Nouvelles, 1 et 4 Avenue de Bois-Préau, 92852 Rueil-Malmaison, France

^b LBE, Montpellier SupAgro, INRA, UNIV Montpellier, Narbonne, France

^c Elsa, Research Group for Environmental Lifecycle and Sustainability Assessment, Montpellier, France

^d CIRAD, UPR Recyclage et risque, F-34398 Montpellier, France

^e CIRAD, UPR BioWooEB, F-34398 Montpellier, France

^f Univ Montpellier, CIRAD, Montpellier, France

^g Chair of Sustainable Engineering, Technische Universität Berlin, Berlin, Germany

^h ITAP, Irstea, Montpellier SupAgro, Univ Montpellier, ELSA Research Group, Montpellier, France

* Corresponding author: ariane.albers@ifpen.fr

Highlights

- Dynamic accounting of SOC from land use activities linked with energy crops for transport biofuels
- The modelling framework contributes to complete GHG inventories including biogenic C and SOC
- Mitigation potentials are sensitive to residue management (C inputs to the soil vs. removal rates)
- Temperature affects organic matter decay and thus mitigation effects
- Soil C sequestration from perennial is higher than that from annual crops

1 **Modelling dynamic soil organic carbon flows of annual and perennial energy crops to**
2 **inform energy-transport policy scenarios in France**

3 **Ariane Albers**^{a, b, c, *}, **Angel Avadí**^{c, d, f}, **Anthony Benoist**^{c, e, f}, **Pierre Collet**^a, **Arnaud Hélias**^{b, g, h}

4 ^a IFP Energies Nouvelles, 1 et 4 Avenue de Bois-Préau, 92852 Rueil-Malmaison, France

5 ^b LBE, Montpellier SupAgro, INRA, UNIV Montpellier, Narbonne, France

6 ^c Elsa, Research Group for Environmental Lifecycle and Sustainability Assessment, Montpellier, France

7 ^d CIRAD, UPR Recyclage et risque, F-34398 Montpellier, France

8 ^e CIRAD, UPR BioWooEB, F-34398 Montpellier, France

9 ^f Univ Montpellier, CIRAD, Montpellier, France

10 ^g Chair of Sustainable Engineering, Technische Universität Berlin, Berlin, Germany

11 ^h ITAP, Irstea, Montpellier SupAgro, Univ Montpellier, ELSA Research Group, Montpellier, France

12 * Corresponding author: ariane.albers@ifpen.fr

13 **Abstract**

14 Low carbon strategies recently focus on soil organic carbon (SOC) sequestration potentials from agriculture and
15 forestry, while Life Cycle Assessment (LCA) increasingly becomes the framework of choice to estimate the
16 environmental impacts of these activities. Classic LCA is limited to static carbon neutral approaches,
17 disregarding dynamic SOC flows and their time-dependent GHG contributions. To overcome such limitation,
18 the purpose of this study is to model SOC flows associated with agricultural land use (LU) and the provision of
19 agricultural substrates to transport biofuels, thus generating dynamic inventories and comparatively assessing
20 energy policy scenarios and their climate consequences in the context of dynamic LCA. The proposed
21 framework allows computing SOC from annual and perennial species under specific management practices
22 (e.g. residue removal rates, organic fertiliser use). The results associated with the implementation of three
23 energy policies and two accounting philosophies (C-neutral and C-complete) show that shifting energy

24 pathways towards advanced biofuels reduces overall resource consumption, LU and GHG emissions. The
25 French 2015 Energy Transition for Green Growth Act (LTECV) leads towards higher mitigation targets compared
26 with business-as-usual (BAU) and intermediate (15BIO) policy constraints. C-neutral results show reduced
27 radiative forcing effects by 10% and 34% for 15BIO and LTECV respectively, but not for BAU. C-complete (i.e.
28 dynamic assessment of all biogenic- and fossil-sourced C flows) results reveal further mitigation potentials
29 across policies, whereof 50%-65% can be attributed to temporal C sequestration in perennial rhizomes. A
30 sensitivity analysis suggests important SOC variations due to temperature increase (+2°C) and changes in
31 residue removal rates. Both factors affect mitigation and the latter also LU, by a factor of -0.56 to +5. This
32 article highlights the importance of SOC modelling in the context of LU in LCA, which is usually disregarded, as
33 SOC is considered only in the context of land use change (LUC).

34 **Keywords:**

35 Biofuels; dynamic life cycle assessment; energy policy scenarios; land use; residue management; SOC modelling

36 **1 Introduction**

37 **1.1 Energy policies and low carbon mitigation strategies**

38 Greenhouse Gas (GHG) emissions need to be reduced by 60% until 2050 (EC, 2018a; UNFCCC, 2018). Between
39 1990 and 2016, GHG emissions of EU-28 showed a relative reduction by 22% in most economic sectors, due to
40 efficiency increases and changes in the energy mix, however, for the transport sector, including international
41 aviation, they have increased by 26% (Eurostat, 2019). In France, 70% of GHG emissions are attributed to fuel
42 combustion, of which about 30% derive from the transport sub-sector (SDES, 2019). Climate-energy policy
43 targets promote a shift towards renewable energy (RE) and advanced biofuels. French policy formulates
44 increasing RE-shares in the energy mix and transport sectors, by 32% and 15% (from a 2012 baseline (MTES,
45 2018)) respectively, as well as reducing GHG emissions by 40% (from a 1990 baseline (IPCC, 2006)).

46 Low carbon strategies include the use of energy crops for producing transport-biofuels, as they are RE carriers
47 considered as carbon neutral GHG inventories. Most of these feedstock consist of dedicated food-crop based
48 annual species (e.g. rapeseed, wheat), as well as lignocellulosic dedicated perennial species and residual
49 matter, among other non-food crop derived biomass such as algae. Advanced second generation (2G) biofuels,
50 i.e. based on perennial grasses, woody residues, and agricultural straw, are increasingly encouraged, as they do
51 not displace food production, regardless of their alleged potential contribution to indirect LUC (Harvey and
52 Pilgrim, 2011).

53 Additional mitigation strategies focus on the potential of carbon sequestration in soils through agricultural
54 practices (Goglio et al., 2015), promoted for instance under the “4 per mille Soils for Food Security and
55 Climate” initiative presented at the 21st Conference of the Parties of the UNFCCC, which resulted in the 2015
56 Paris Climate Agreement (CGIAR, 2018; INRA, 2019; Minasny et al., 2017; Zanella et al., 2018). This initiative
57 faces nonetheless some criticism on the extent to which soil can sequester carbon (e.g. White et al. 2018) and
58 the concept of soil carbon sequestration itself, as the release of nutrients is one of the key functions of soil
59 organic matter (SOM) (Lehmann and Kleber, 2015). Therefore, the dynamic of soil organic carbon (SOC), as

60 influenced by biomass production and use, needs further research when modelling climate benefits of future
61 energy scenarios.

62 Prospective bottom-up energy system models are instruments assessing policy scenarios and their effects on a
63 (sub-)sector, by means of linear programming and optimisation (Loulou et al., 2016). Scenario simulations from
64 these models are built on least cost and low carbon energy pathways, involving technological innovation,
65 efficiency and RE from fossil and biomass sources. The dynamic of SOC and LU are however not considered in
66 energy system models (Frank et al., 2015).

67 **1.2 Soil organic carbon modelling and applications in life cycle assessment**

68 SOC is the main component of SOM, accounting for 55-60% by mass, divided among three pools:
69 fast/labile/active (turnover time of 1-2 years), intermediate (turnover time of 10-100 years), and
70 slow/refractory/stable (turnover time of >100 years) (FAO, 2017). The turnover rate plays a key role in the
71 functioning (e.g. health) of the soil ecosystem, as well as on climate change, as C is eventually released to the
72 atmosphere, as it undergoes continuous decomposition in the soil under influence of soil fauna activity
73 (Kwiatkowska-Malina, 2018; Lehmann and Kleber, 2015; Campbell and Paustian, 2015; FAO, 2017). Several
74 physical and biochemical mechanisms may influence the decomposition rate, and these mechanisms can be in
75 turn influenced by management (e.g. to increase C sequestration) (Wiesmeier et al., 2019; Zomer et al., 2017).

76 In general, SOC models take into consideration soil temperature, water, and clay content; as main drivers for
77 changes in C stocks (Bockstaller and Girardin, 2010; Ci et al., 2015; FAO, 2017; Han et al., 2018; Zhong et al.,
78 2018). They are usually based on the assumption that SOM decomposes following first order kinetics (Luo et
79 al., 2016; Smith et al., 2012), initially proposed in the 1945 pioneering model from Hénin and Dupuis (Henin
80 and Dupuis, 1945; Shibu et al., 2006), where the decomposition rate constant corresponds to the pedoclimatic
81 condition-dependent annual mineralisation rate. Mineralisation coefficients can be estimated from measured
82 data (e.g. Delphin 2000) or modelled (Benbi and Richter, 2002; Bockstaller and Girardin, 2010), and are often
83 available in the literature (e.g. Gobin et al. 2011).

84 SOC modelling in agriculture, livestock, climate mitigation and LCA are carried out by means of different
85 methods, depending on the purpose of the study, data availability and spatial scales (i.e. site-specific, site-
86 dependent or site-generic variables). Common classifications involve three levels of complexity (Bolinder et al.,
87 2006; Campell and Paustian, 2015; FAO, 2018; Goglio et al., 2018, 2015; Shibu et al., 2006; Smith et al., 2012): i)
88 analytical/empirical models, mostly based on the factors from IPCC Guideline for National GHG Inventories
89 (IPCC, 2006), ii) process-oriented/conceptual models, with increasing complexity according with the number of
90 pools considered, and iii) ecosystem/summary models, i.e. multi-compartment models involving sub-models
91 such as plant growth, dynamic crop-soil-crop models etc.

92 Analytical modelling methods are based on two main rationales: gain-loss, where processes altering C content
93 of pools are considered, and stock-difference, most common in LCA, where C stocks in pools are measured at
94 two points in time (Benoist and Bessou, 2018; IPCC, 2006). Empirical models, such as the Campbell model
95 (Campell and Paustian, 2015), use two functions to describe changes in SOC: one to model C dynamics
96 associated with organic inputs (i.e. residues) and another for the decomposition of pre-existing SOC (Liang et
97 al., 2005; Smith et al., 2012). These models have also been used to assess the C sequestration potentials of
98 specific crops, such as the one proposed in Grogan and Matthews (2002) for energy crops (short rotation
99 coppice willow). Other analytical models include the two-compartment (i.e. active and stable) Introductory
100 Carbon Balance Model (ICBM) (Andrén and Kätterer, 1997) and variations of the three-compartment model
101 first presented by Andriulo et al., (1999a), such as the AMG model (Clivot et al., 2019; Duparque et al., 2013;
102 Saffih-Hdadi and Mary, 2008). The use of such models requires site-dependent coefficients (e.g. degradation
103 rates; effects of clay, humidity and temperature). Complex dynamic models, on the other hand, aim at
104 answering questions beyond C or N sequestration: their goal is to predict the performance of specific
105 agricultural systems involving site-specific (i.e. local) calibrations.

106 LCA generally requires simple, site-generic models, which are useful under a variety of conditions and require a
107 minimal amount of input data. Two models widely used in LCA, the monthly time-stepped C-TOOL (Petersen,
108 2003) and the daily to annually time-stepped RothC (Coleman and Jenkinson, 2014), demand a larger number

109 of input parameters than ICBM or AMG models (Campbell and Paustian, 2015; Goglio et al., 2015). Complex
110 agro-ecosystem models such as CANDY, CENTURY, CERES-EGC, DAYCENT, DAISY, DNDC and STICS have been
111 occasionally used in LCA (Brilli et al., 2017; Campbell and Paustian, 2015; Goglio et al., 2015; Gueudet, 2012),
112 but the required level of expertise and data hinder their widespread applicability.

113 **1.3 Land activities in the context of soil organic carbon modelling**

114 In LCA, two types of activities are modelled in relation with SOC, namely LUC and LU, the latter referring to use
115 of a land over time not involving LUC. LUC is associated with “transformation” and LU to “occupation”, two
116 keywords used in LCA software to identify these two elementary flows. Depending on methods and data
117 availability, land management changes (LMC) can be modelled as either transformation or occupation
118 processes (Benoist and Bessou, 2018). LMC-related agricultural practices potentially affecting SOC dynamics
119 include management of agricultural residues, organic fertilisation and the selection of high-biomass crops and
120 rotations (Goglio et al., 2015, 2014).

121 The original ILCD handbook (EC-JRC, 2010) recommended a widely used single-indicator model for calculating
122 the impacts of transformation and occupation, based on changes in soil quality, expressed in terms of SOM
123 (Milà i Canals et al., 2007a, 2007b). More recently, the Product Environmental Footprint (EC, 2018b; Sala S. et
124 al., 2019) suggested the multi-indicator models LANCA (Bos et al., 2016) and latest LANCA v2.5 (Horn and
125 Maier, 2018). Regarding SOC modelling itself, mostly characterisation factors and simple models are used in
126 LCA, yet no recommended or consensus model exists (Goglio et al., 2018, 2015). For instance, the PEF
127 guidelines (EC, 2018b) recommend the PAS 2050 approach (BSI, 2011) to be used for all C emissions and
128 removals arising from LUC, but PAS 2050 does in turn recommend using IPCC methods (for LCIs) and reporting
129 SOC-related results separately. The IPCC approaches for SOC modelling (Tiers 1 and 2, and characterisation
130 factors), include only the topsoil (first 30 cm), thus disregarding intermediate and stable pools.

131 The UN Environment (formerly UNEP-SETAC) Life Cycle Initiative recommends the same SOM-based approach
132 to occupation and transformation of land as IPCC, yet it also recommends a specific method for SOC impacts on

133 C sequestration and climate change (Koellner et al., 2013). This method, described in Müller-Wenk and
 134 Brandão (2010), provides factors for C losses to air, from an initial stock in soil (estimated per biome),
 135 associated to various types of occupation and transformation. It is one of the few approaches, together with
 136 Schmidinger and Stehfest (2012), a method under development (Benoist and Cornillier, 2016), and project-
 137 oriented methods based on IPCC (e.g. under the Kyoto Protocol's Clean Development Mechanism,
 138 <https://cdm.unfccc.int/methodologies/index.html>), considering the impacts on climate change via C
 139 sequestration and release of both transformation and occupation of soils (Benoist and Bessou, 2018). Table 1
 140 summarises the features of some of these modelling approaches used in LCA.

141 Table 1. Comparison of recommended static modelling approaches for calculating soil quality SOM/SOC changes
 142 associated with LU (occupation) and LUC (transformation) in LCA

Method	Recommending guideline	Land activities included	Usefulness for LCIA	Notes
SOM/SOC change (Brandão and Milà i Canals, 2013; Milà i Canals et al., 2007a, 2007b)	International Reference Life Cycle Data System (EC-JRC, 2010)	T+O	CF available, limited linking to AoP	Informing soil quality, site-dependent or -generic, but not climate change
LANCA (Beck et al., 2010; Bos et al., 2016; Horn and Maier, 2018)	Product Environmental Footprint Category Rules (EC, 2018b)	T+O	CF available	Informing soil functions, data intensive, suitable for site-dependent or generic assessment
SALCA-SQ (Oberholzer et al., 2012, 2006)	ecoinvent v2 (Nemecek et al., 2011; Nemecek and Kagi, 2007)	O	CF available, limited linking to AoP	Informing soil properties and treats, site-dependent or site-specific (plot level)
Müller-Wenk and Brandão (2010)	UNEP-SETAC (Koellner et al., 2013)	T+O	CF available	Informing climate change, site-generic (6 biomes over the world)
PAS 2050 standard (BSI, 2011) and IPCC Guideline for National GHG Inventories (IPCC, 2006)	Product Environmental Footprint Category Rules (EC, 2018b)	T	N/A	Dynamic modelling in the context of CDM methodologies, but site-dependent

Acronyms. AoP: Area of Protection, SOC: Soil Organic Carbon, SOM: Soil Organic Matter, T: Transformation; O: Occupation, LCIA: Life Cycle Impact Assessment, CF: characterisation factors, GHG: Greenhouse Gas, CDM: Kyoto Protocol's Clean Development Mechanism
 Sources: Benoist and Bessou (2018)

143 Regarding biofuels, the effect of LU and LUC on soil C dynamics, as well as that of residue management
 144 practices (i.e. removal rates of residues exploited as RE carriers), are of key interest (Brandão et al., 2011;
 145 Caldeira-Pires et al., 2018; Smith et al., 2012). The overall potential C sequestration of energy crops has been
 146 computed, and estimated to be positive (Lemus and Lal, 2005; Mi et al., 2014; Zang et al., 2018). Moreover, the

147 need for time dynamic SOC modelling in LCA has been highlighted (Brandão et al., 2013, 2011; Sommer and
148 Bossio, 2014). A first effort in that direction is the approach to include SOC changes in LCA proposed by
149 Petersen et al. (2013), which relies on the Bern Carbon Cycle Model to determine degradation curves, the
150 superposition of which allows, by mass-balance, to estimate the amount of C remaining in soils by the end of
151 the assessment time horizon (TH).

152 **1.4 Goal and scope of the study**

153 Based on such environment of evolving SOC modelling approaches and applications in LCA, the goal of this
154 work is to propose a dynamic SOC modelling approach for life cycle inventories associated with LU and
155 agricultural substrates to biofuels. The proposed approach would contribute to overcoming identified gaps of
156 SOC modelling in LCA, namely, the consideration of: SOC associated with LU, SOC dynamic within a given
157 reference TH, and the need for accessible SOC models in LCA. Furthermore, the resulting dynamic SOC
158 inventories are integrated into a dynamic model-coupling framework with a partial-equilibrium model (PEM)
159 as proposed in Albers et al., (2019a), to comparatively assess future energy-transport scenarios and climate
160 change consequences associated with SOC. A key aspect of the proposed approach is its dynamic
161 representation of SOC associated with the dynamic technical flows of the system, to more accurately estimate
162 climate change impacts.

163 The functional unit in this study represents the annual energy demand, in MJ, over the prospective PEM
164 simulation period (2019 to 2050), defined per policy constraint, here to satisfy the energy consumption of
165 transport end-users, in this study referring to bioethanol and biodiesel from agricultural energy crops.

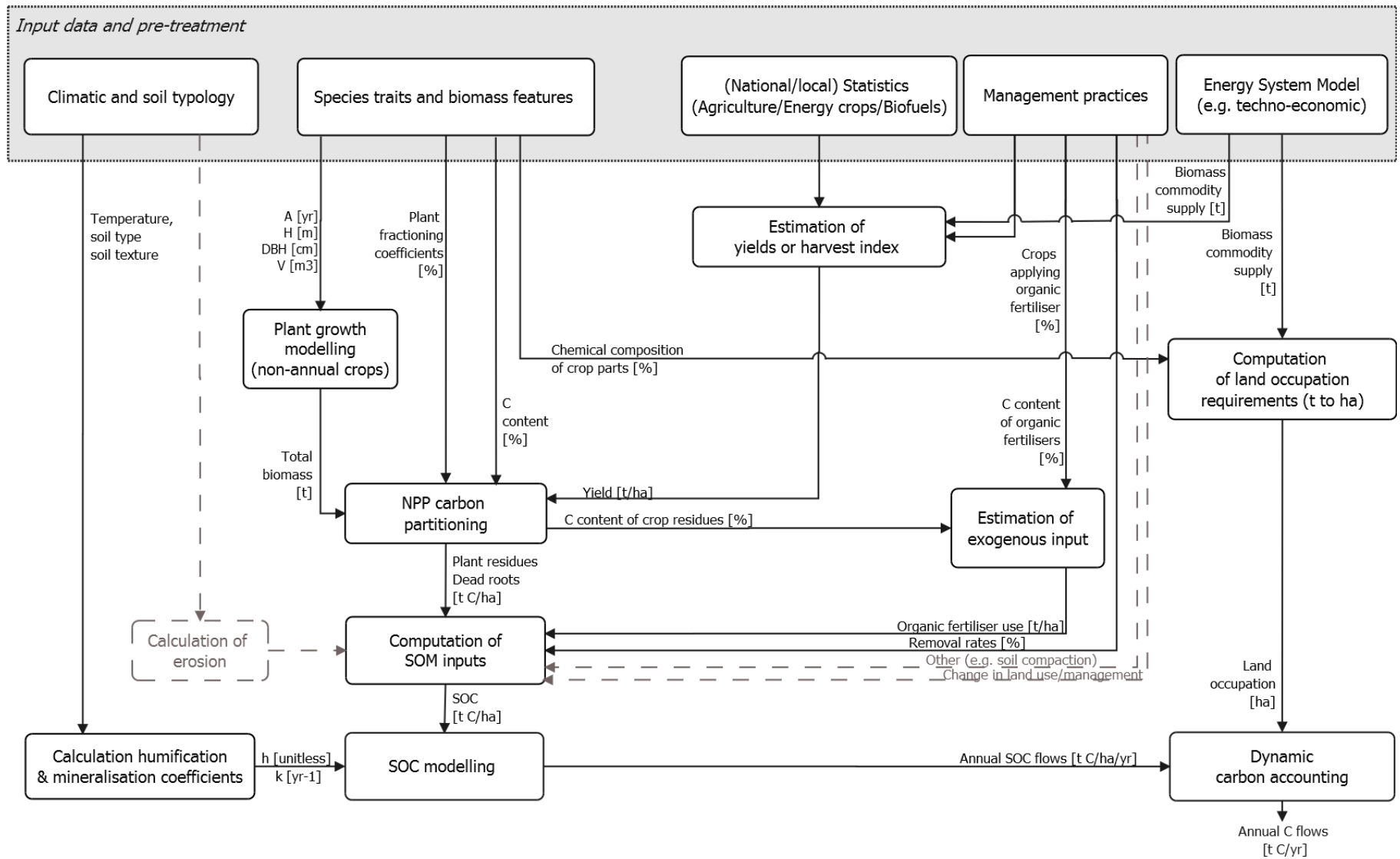
166 **2 Material and methods**

167 The construction of dynamic SOC inventories associated with energy policy scenarios and LU, follows the
168 model-coupling framework specified in Fig. 1. The framework allows computing dynamic SOC flows from
169 agricultural annual and/or perennial energy crops under specific (yet variable) management practices (e.g.

170 residue removal, or organic fertiliser use). The SOC model includes C inputs to the soil stemming from
171 aboveground (AG) and belowground (BG) plant compartments, as well as from exogenous (EX) sources (i.e.
172 organic fertilisers). Site-dependent coefficients, such as temperature and soil characteristics, relate to the crop
173 cultivation in France, except for soybean, which is assumed to be imported from Brazil.

174 Firstly, the technical flows obtained from the energy system model (it could have been any other demand
175 model) are exported to a) inform SOC modelling on the biomass commodity supply, b) compute LU
176 requirements, and c) represent the results specific to two selected transport-biofuel (bioethanol and biodiesel)
177 pathways per biomass commodity. Secondly, annualised “C-complete” balances are built by combining
178 dynamic accounting of biogenic- (here referring to SOC flows) and fossil- (referring to C neutral flows without
179 biogenic flows) sourced CO₂ elementary flows, which are subsequently assessed with time-dependent
180 characterisation factors in the context of dynamic LCA (Levasseur et al., 2010). This study does not represent a
181 complete LCA, as it solely focuses on modelling dynamic life cycle inventories of SOC and their climate change
182 consequences.

183



184

185 Fig. 1. Coupling diagram of energy system and soil organic carbon modelling for dynamic carbon accounting (Acronyms: A: Age, C: Carbon content, DBH: Diameter
 186 Breast Height, H: Height, h: Humification coefficient, k: Mineralisation coefficient, NPP: Net Primary Productivity, SOC: Soil Organic Carbon, V: Volume)

187

188 **2.1 Processing model outputs from the energy system model**

189 **2.1.1 Demand model informing policy scenarios for the transport sub-sector**

190 For this study, we exported energy crop commodity outputs from the TIMES-MIRET partial-equilibrium energy
191 system model (Lorne and Tchong-Ming, 2012), over the simulation period 2019 - 2050. TIMES-MIRET is a
192 bottom up PEM, also referred to as techno-economic model, covering the energy-transport sector of
193 metropolitan France. Further specifications on the model were previously introduced in Albers et al. (2019a).
194 The TIMES-MIRET calibration is based on the 2009 EU Directive and National Energy Plan, with climate targets
195 by 2020 serving as a reference in the business-as-usual (BAU) policy scenario. BAU is contrasted with new
196 targets by 2030 from the 2015 French Energy Transition for Green Growth Act for the transport sub-sector. The
197 new constraints are a 15% renewable energy share in the transport-subsector and a maximum of 7% 1G
198 biofuels (here analysed with the 15BIO scenario), as well as a 30% reduction of fossil fuel and intermediate
199 targets for advanced biofuels (here analysed in the LTECV scenario) (MTES, 2018).

200 **2.1.2 Biomass-to-biofuel commodities and land use**

201 Biomass-to-biofuel pathways, retrieved from the PEM, depend on the policy constraints given to the model.
202 The following biomass commodities flows [kt] were considered: first generation (1G) crop-based starch (wheat,
203 rapeseed, maize and triticale), oil (rapeseed, sunflower and soybean), sugar (sugar beet), as well as second
204 generation (2G) residual lignocellulosic straw (wheat, rapeseed, maize and triticale) and dedicated
205 lignocellulosic perennial grasses (miscanthus and switchgrass as a proxy for dedicated lignocellulosic biomass).
206 Other commodities (e.g. algae, yeast, palm oil, sewage sludge, and spent cooking oil) are excluded due to their
207 comparatively low to null contributions to the overall biofuel transport sector in the three analysed policy
208 scenarios. The biofuel pathways included in this study refer to transport bioethanol and biodiesel.

209 We computed the LU requirements [ha yr^{-1}] in terms of the equivalent agricultural area. Such conversion is
210 based on statistics and literature on agricultural data of potential yields per area [$\text{t}\cdot\text{ha}^{-1}$] revealing the amount
211 of crop product that is exported from the field and the chemical composition of the harvested crop product,

212 determining its starch, sugar or oil contents [%]. Residues (straw) are computed based on the residue yield of
213 the whole plant times the residue removal rate (if any), while dedicated perennials represent 100% of the
214 lignocellulosic commodity. Detailed specification on the computation and methods used for biomass-to-
215 biofuel, LU and GHG emission conversion are provided in the Supplementary Material.

216 **2.2 Dynamic soil organic carbon modelling**

217 We adapted the relatively simple, yet appropriate for modelling dynamic inventories, SOC model of Hénin and
218 Dupuis (1945). The model runs with a time step of one year compatible with the time-dependent climate
219 change characterisation. Hénin and Dupuis' model is based on the interaction of C between two soil
220 compartments: i) fresh organic matter input from AG (crop residues) and BG plant parts (dead roots and
221 rhizomes), as well as exogenous organic inputs (e.g. soil amendments/fertilisers), and ii) the active pool (soil
222 layer up to 30 cm depth) (see Supplementary Material). The C balance represents the difference between the
223 dynamic C input [$t \text{ C} \cdot \text{ha}^{-1}$] from a flow of organic matter (m) entering the active pool at a given time (t_0), as well
224 as the losses from C output flows (here as CO_2 flows) determined by instant releases determined by the
225 isohumic coefficient (h) and the gradual decay determined by the mineralisation coefficient (k). The model has
226 been developed into a long-term SOC model, referred to as the AMG model (Andriulo et al., 1999), undergoing
227 continuous refinements (latest version introduced in Clivot et al. (2019)). AMG accounts for C stocks in the
228 upper layers (≤ 30 cm) and stable deeper layers (> 30 cm). It has been integrated in the STICS model (Saffih-
229 Hdadi and Mary, 2008) and implemented into the SIMEOS-AMG tool (Bouthier et al., 2014).

230 For the model coupling (here with an energy model), it is required to assess the technical flows of a product
231 system (here biofuels) for any given calendar simulation year, independent from C stocks or C losses from
232 previous LU or LUC. In contrast to the long-term AMG model, we aim at modelling the added C to the soil given
233 by the technical flows and its time-dynamic decay within the active pool (i.e. the annual difference between
234 the remaining C from a single-year input and the C releases over time until the SOC balance equals zero). Thus,
235 initial stable C stocks from long-term crop cultivation systems associated with the same LU over several

236 consecutive years are not modelled and it is assumed that the stable pool does not change over several
237 centuries (Kwiatkowska-Malina, 2018; Shibu et al., 2006).

238 The modelling of the soil C balance is computed with Eq. 1 , according with Hénin and Dupuis (1945), however
239 fractioning the C input from m into AG (crop residues including exogenous matter) and BG (root system)
240 compartments. The integral for the net annual flows for AG and BG are given in Eq. 2 and
241 Eq. 3 respectively:

$$C_{AP} = C_{AG} + C_{BG} \quad \text{Eq. 1}$$

$$C_{AG}(t_0) = m_{AG}h \quad \text{Eq. 2}$$

$$\frac{dC_{AG}}{dt} = -kC_{AG}$$

$$C_{BG}(t < t_{RL}) = m_{BG} \quad \text{Eq. 3}$$

$$\frac{dC_{BG}}{dt} = \begin{cases} 0, & \text{when } t < t_{RL} \\ -k C_{BG}, & \text{when } t \geq t_{RL} \end{cases}$$

242 where C_{AP} [$\text{t C}\cdot\text{ha}^{-1}$] is the carbon content in the active pool from AG and BG compartments, m is the added
243 carbon at time t [yr], RL the rotation length [yr], h [unitless] is the humification coefficient, and k [yr^{-1}] the
244 mineralisation coefficient. The rationale behind dividing C_A into AG and BG is the dynamic character of
245 perennial grasses, as the rhizomes remains in the soil in the long-term (i.e. C is stored over the entire
246 cultivation/ RL period), while AG residues contribute to annual C inputs (i.e. AG biomass is harvested every year
247 like annual crops) (Beuch et al., 2000). The long-term model, on the other hand, does not allow assessing
248 perennial species (Clivot et al., 2019).

249 2.2.1 Humification coefficient

250 The isohumic coefficient h (by some authors also referred to as k_1) represents the ratio between the added
251 SOM contributing to SOC increase and the total amount of the added SOM (Hénin and Dupuis, 1945). It thus
252 represents the fraction of SOM transformed into humified C (i.e. available to plants), while the remaining C is

253 released to the atmospheric pool, via mineralisation (Kwiatkowska-Malina, 2018). High h values mean that the
254 organic matter decomposes easily (e.g. 15% for straw compared with up to 70% for some soil amendments) (Le
255 Villio et al., 2001). For this study, h values and C contents per crop type and EX matter were taken from the
256 literature (Supplementary Material).

257 **2.2.2 Mineralisation coefficient**

258 The initial SOC stock is continuously reduced by mineralisation, over time (i.e. a flow, represented by positive
259 emissions), until the net balance reaches zero. The mineralisation coefficient k (also referred to as k_2 by some
260 authors) represents the annual decay of SOM as GHG emissions, such as CO₂, and the release of nutrients into
261 plant-assimilable forms, and depends heavily on soil type, soil characteristics, and other pedoclimatic
262 conditions. Saffih-Hdadi and Mary (2008) demonstrated that C mineralisation of crop residues (and by
263 extension of any exogenous organic matter) is driven by the substrate quality rather than by the soil type
264 (under the same humidity and temperature conditions). The C:N ratio also plays a key role in SOM
265 mineralisation (Nicolardot et al., 2001), but this parameter is not directly used in this model, as its influence is
266 captured in the humification coefficient.

267 In France, the mean annual mineralisation constant rate is often estimated at 2% (Frisque, 2007; Le Villio et al.,
268 2001; UNIFA, 1998). A review (see the Supplementary Material) of several site-specific studies (with k
269 calibrated to specific locations) indicated a range between 0.7% and 9%, with mean values at 4%. For
270 computing k , the updated method proposed in the AMGv2 model (Clivot et al., 2019), takes under
271 consideration soil mean temperature, clay and calcium carbonate (CaCO₃) contents. Our k estimates excluded
272 soil moisture, pH and C/N ratio, as the scope of the study disregards site-specific parameters, focusing primarily
273 on the C flows. Soil temperature, clay and CaCO₃ content are the key parameters in this study, providing close
274 approximations for a usable mineralisation rate. We computed k for eight climate types in France, referring to
275 the classification by Joly et al. (2010), for which a dominant soil type can be roughly assigned. For the model
276 coupling, we chose climate Type 3 (Central France) featuring a mean temperature of 11°C and mean clay
277 content of 16.8%, as this climate type represents an important agricultural area for cereals and oil crops. For

278 the imported soybean, we used the same method, based on the reference soil temperature of 27°C,
279 representing about 2°C higher for surface soils in soybean cropland in Mato-Grosso, Brazil (Nagy et al., 2018).
280 All specifications are provided in the Supplementary Material.

281 **2.3 Modelling carbon inputs from aboveground, belowground and exogenous matter**

282 The net C inputs to the soil dependent on management practices defining removal/export rates from the AG
283 compartment (crop products, residues) and BG compartment (rhizomes and roots), as well as the incorporation
284 of non-mineral exogenous matter (organic fertiliser). Therefore, methods were adapted to model the
285 partitioning of C in the different crop fractions, to determine what proportion of AG and BG plant are
286 incorporated in the soil and whether EX matter is added.

287 **2.3.1 Rhizomes growth and carbon fixation of perennial grasses**

288 Dynamic growth and carbon sequestration of annual crops are commonly excluded from dynamic carbon
289 modelling, as their C fixation and release flows occur within one year, equivalent to carbon neutrality (Guest et
290 al., 2013). The same applies to the AG perennial grasses, harvested annually. However, growth dynamics of the
291 BG biomass fraction require an additional modelling step, given that the C fixation in the rhizomes occurs over
292 several years, in contrast to annual crops.

293 We considered the miscanthus (*Miscanthus x giganteus*) and switchgrass (*Panicum virgatum*), which are
294 perennial rhizomatous C4 grasses. These grasses have extensive root systems, which may increase in the long-
295 term (Agostini et al., 2015). However, dynamic growth models for root system are not accessible, as they tend
296 to be very complex and species-specific (Dupuy et al., 2010). A meta-analysis by Agostini et al. (2015)
297 highlighted that the biomass growth from the BG compartment and the C inputs to the soil are mainly based on
298 several single observations with variable stand age, depths and sampling frequencies, making it difficult to
299 model the time series of the root system. Yet, it has been demonstrated that the C fixation increase with
300 increasing cultivation period (Arevalo et al., 2011; Rehbein et al., 2015).

301 Rehbein et al. (2015) calculated the miscanthus-derived C for different soil depths/layers up to 100 cm and
302 showed that the C stock increased linearly with increasing time ($R^2 = 0.8$, $P < 0.001$) in the top soil (≤ 10 cm) and
303 deeper soil layers (0-100 cm), whereas 60 to 80% of the C is associated to the top soil. Based on the results
304 from Rehbein et al. (2015) and meta-analysis from Agostini et al. (2015), we distributed the total C over the
305 entire rotation length linearly to represent the rhizomes growth and C fixation in the biomass. Consequently,
306 the time-dependent C_{BG} inputs to the soil (Eq. 3) from miscanthus and switchgrass take place after the end of
307 the rotation length at 20 and 15 years respectively. Both C fixation and SOC release flows are allocated
308 accordingly.

309 **2.3.2 Plant fractioning and carbon partitioning**

310 For computing the C inputs to the soil from AG and BG compartments, the approach of Bolinder et al. (2007),
311 applied in other studies (Clivot et al., 2019; Wiesmeier et al., 2014), was adopted. The authors conceptualise
312 the C input to the soil as a proportion of net primary productivity (NPP), summing up four plant fractions per
313 unit of area [$t \cdot C \cdot ha^{-1}$]:

- 314 ▪ C_P : the C in the agricultural product (P) in the AG (e.g. seed, grain, perennial grasses, and forage crops)
315 or BG (e.g. tuber) compartments, representing the primary economic value, not incorporated into the
316 soil.
- 317 ▪ C_S : C in the residual (S) AG fraction (e.g. straw, stover) incorporated into soil after harvest.
- 318 ▪ C_R : C in root (R) BG tissue (rhizome), physically recoverable plant materials (excluding products such as
319 tubers from sugar beet), mostly incorporated in the soil after harvest.
- 320 ▪ C_E : C in extra-root (E) matter (rhizome deposition), involving root exudates and plant materials
321 physically not easily recoverable, mostly incorporated in the soil after harvest.

322 C partitioning per plant fraction and per crop follows the method from Bolinder et al., (2007), including data
323 from the literature (mean annual yield per crop and relative C allocation coefficients), both presented in the
324 Supplementary Material. The C inputs to the soil depend on the annual yield estimates at field scales, obtained
325 from statistics and literature. These values can be adapted to site-specific evaluations.

326 **2.3.3 Estimation of exogenous inputs**

327 Exogenous C inputs consist of added organic matter, under the form of amendments and fertilisers (Saffih-
328 Hdadi and Mary, 2008). Based on French statistics on crop production (surfaces, yields) and organic fertiliser
329 use (AGRESTE, 2019, 2014, 2011), as well as on the composition of French organic fertilisers (Avadí, 2019),
330 average French fertilisation practices for each crop of interest were constructed. For Brazilian soybean, data
331 was retrieved from FAO (2004).

332 **2.4 Variations of carbon inputs to the soil**

333 Not all the C embedded in plant fractions is returned to the soil. The net C inputs from AG, BG and EX matter
334 depend on agricultural management practices. Consequently, four different scenarios are analysed and
335 contrasted in this study, which could eventually be associated with residue management practices:

- 336 ▪ Scenario S1_TOT: Total C inputs to soil (aboveground + belowground + exogenous carbon)
- 337 ▪ Scenario S2_AG: C from aboveground plant residues
- 338 ▪ Scenario S3_BG: C from belowground plant residues
- 339 ▪ Scenario S4_EX: C from exogenous matter

340 The resulting scenarios are based on the origin of C from different plant fractions (AG and BG) and EX matter,
341 whereas S1_TOT represents the sum of all added C to the soil. These scenarios represent highly contrasted
342 extremes of management practices. In reality, these practices are likely to be more nuanced (e.g. partial
343 combinations of AG, BG, EX added to the soil). The high contrast allows identifying the origin of C and their
344 proportional contributions to the total SOC input.

345 We assumed that the total C_p is harvested. However, C_s , C_R and C_E inputs are adjusted with correction factors
346 ranging between 0 (no C input) and 1 (100% C input) to specify the C plant proportion added to the soil (more
347 details provided in the Supplementary Material). In France, common C_s removal rates from cereals and oily
348 seeds are in the order of 0.5, while for vegetables, protein crops and perennials they are in the order of 1,
349 whereas C_s from switchgrass is zero (ADEME, 2017). C_R and C_E are assumed to be wholly incorporated into the
350 soil (except for sugar beet root, which is exported from the fields).

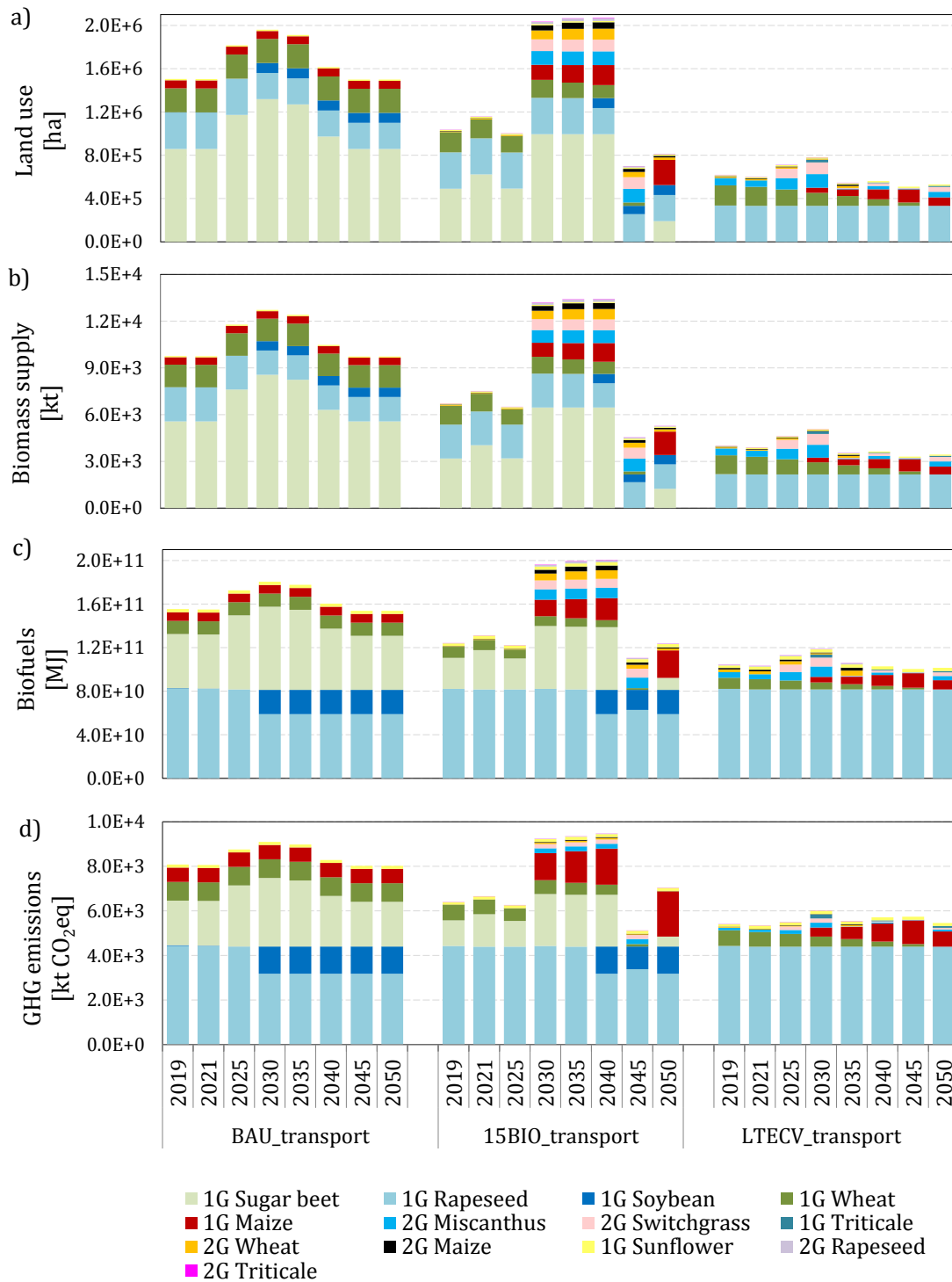
351 **3 Results and discussion**

352 **3.1 Policy scenario simulations from the partial-equilibrium with static GHG emissions**

353 Fig. 2 shows a comparative overview of the three analysed policy scenarios (BAU, 15BIO and LTECV) of the
354 transport sub-sector from 2019 to 2050, analysed with the PEM, denoting LU requirements [ha], biomass
355 commodity supply [kt], final energy supply [MJ], and associated GHG emissions [kt CO₂-eq] of the simulations
356 represent the pathways of bioethanol and biodiesel demand only.

357 A general comparison among the three policy scenarios shows a clear shift from 1G to 2G energy carriers for
358 the transport sub-sector, particularly evident for the LTECV scenario. The shifting energy-pathways reduce the
359 overall resource consumption and LU demand, particularly for 1G energy crops, that consequently reduce the
360 GHG emissions to meet the mitigation targets. It is noticeable that the prospective evaluations assume
361 increased number of passengers per km driven per transport means, and thus reduced future fuel demand. The
362 15BIO scenario shows sudden increases between the years 2030 and 2040, responding to the constraint of
363 limiting 1G share to 7% from 2020, remaining effective in the 2030s, concerning the multi-annual energy
364 program in the transport sector. The scenario simulations return to a new equilibrium, as no further constraints
365 are specified for advanced biofuels, yet the values remain under BAU evaluations. In contrast, LTECV takes into
366 account all policy constraints from the French law for the transport sub-sector, such as intermediate targets for
367 advanced biofuels and 30% reduction of fossil fuels in the final net energy share.

368 Results for LU requirements (Fig. 2a), reveal the equivalent agricultural area requirements associated with the
369 biomass commodity supply of 1G and 2G transport biofuels. A comparison with BAU, shows that while LU for
370 1G decrease, they increase for 2G due to the shifting energy pathways towards more advanced biofuels. Yet,
371 the overall LU decreases per policy scenario with 50%, 41% and 9% for BAU, 15BIO and LTECV respectively. The
372 proportion of the derivative commodities (starch, sugar, oil) to the equivalent harvested energy crop yields
373 vary considerably between 18% and 64%, and therefore represent higher equivalent agricultural area demand,
374 compared with the residual and dedicated lignocellulosic commodities.



375

376 Fig. 2. Policy scenario simulations (BAU, 15BIO, LTECV) linked with first (1G) and second (2G) generation bioethanol and
 377 biodiesel pathways in terms of a) land use requirements in ha, b) biomass commodity supply in kt, c) equivalent energy
 378 supply in MJ, and d) associated Greenhouse Gas emissions in kt CO₂-eq

379 The biomass commodity supply (Fig. 2b) in the BAU policy —which does not follow the multi-annual energy
 380 program for the transport sub-sector— accounts for dedicated 1G annual crops only, dominated by sugar beet
 381 (60%), rapeseed (17%), and wheat (13%). 15BIO policy increases the 2G-share by 15%, yet sugar beet (44%),

382 rapeseed (22%) and wheat (9%) remain the main supply sources. The LTECV policy further increased the 2G-
383 share up to 17%, of which perennial grasses (miscanthus and switchgrass) contribute to 90%. 1G soybean and
384 1G sugar beet would be displaced completely; yet 1G rapeseed (55%) and wheat (17%) will remain the main
385 supply sources.

386 The net final energy supply (Fig. 2c) represents the bioethanol and biodiesel yield per dry matter of the
387 commodity. Conversion efficiencies vary strongly among the different renewable energy carriers, whereby
388 oleaginous crops have higher yield efficiencies. The main contributor to the net biodiesel supply will
389 increasingly be rapeseed oil with up to 41%, 49% and 77% for BAU, 15BIO and LTECV respectively, and for
390 bioethanol sugar beet with up to 36% and 23% in BAU and 15BIO respectively (yet 0% for LTECV). With the
391 upcoming technological innovation for advanced biofuels, LTECV scenarios showed that advanced biofuels
392 (involving synthetic biofuels) will play a major mitigation role, with up to 10% share in the net final energy.

393 The GHG emission estimates (Fig. 2d) linked with fossil fuels only are based the EC JRC well-to-wheel method
394 (Edwards et al., 2014), for bioethanol and biodiesel and the static IPCC GWP metric. The highest mitigation
395 targets are achievable by means of the LTECV scenario. All emissions in the BAU scenario derive from 1G
396 biofuels, whereas 4% and 3% originate from 2G in 15BIO and LTECV respectively. 1G source are the main
397 contributors to GHG emissions, particularly rapeseed oil (up to 43%, 53% and 73% for BAU, 15BIO and LTECV
398 respectively) and sugar beet (up to 28% and 19% in BAU and 15BIO respectively). The lower impact
399 contributions from 2G biofuels are due to reduced emission factors in $\text{g of CO}_2\text{eq}\cdot\text{MJ}^{-1}$, as compared with
400 conventional fuels and 1G biofuels.

401 **3.2 Parameters for soil organic carbon computation**

402 Table 2 provides an overview of data and coefficients used to compute the C inputs to the soil, associated with
403 crop C content, humification coefficients, yields, carbon partitioning per relative plant fraction, NPP, and
404 exogenous inputs, per ha, at field scales. C fractioning among plant parts and C partitioning from NPP are
405 calculated here from annual yield estimates at field scales, per ha. For miscanthus, for which few data is

406 available, dry matter yields range between 16.1 and 28.5 in France (AGRESTE, 2019; Strullu et al., 2014) and
407 globally between 14.8 and 33.5 (Rehbein et al., 2015). We used the mean 22.8 t DM ha⁻¹ based on measured
408 values by Strullu et al. (2014). EX matter represents mean French agricultural practices regarding fertilisation of
409 cultivation of energy crops. The mineralisation coefficients resulted in 0.1176 for French cereals and oily seeds
410 and 0.0733 for Brazilian soybean, based on the regional mean temperature estimated at 25°C and a clay
411 content of about 43%. The computation, underlying data and assumptions are further detailed in the
412 Supplementary Material.

413 Table 2. Isohumic coefficient (h), carbon (C) content, carbon partitioning from net primary productivity (NPP), and mean French agricultural practices regarding
 414 fertilisation of energy crops and exogenous inputs

Crops and residues	Yields [t·ha ⁻¹]	Isohumic coefficient (h) [unitless]	C content [t·t ⁻¹]	Carbon partitioning per plant fraction (calculated)				NPP [t C·ha ⁻¹]	Fertilisation of cultivation of energy crops (calculated)									
				C _P [t C·ha ⁻¹]	C _S [t C·ha ⁻¹]	C _R [t C·ha ⁻¹]	C _E [t C·ha ⁻¹]		Mineral N [kg·ha ⁻¹]	Cattle effluents [t·ha ⁻¹]	Poultry effluents [t·ha ⁻¹]	Swine effluents [t·ha ⁻¹]	Compost [t·ha ⁻¹]					
Maize	11.980	a	0.193	e	0.414	i	4.957	5.369	2.959	1.967	15.251	l	133	11.069	0.519	1.513	1.410	m
Rapeseed	3.655	a	0.244	f	0.502	i	1.901	10.231	3.393	2.238	17.763	l	169	3.989	0.187	0.545	0.508	m
Wheat	6.408	a	0.193	f	0.475	i	3.046	4.354	1.697	1.124	10.220	l	169	0.819	0.038	0.112	0.125	m
Triticale	5.501	a	0.125	e	0.475	i	2.615	5.088	1.428	0.925	10.056	l	107	5.265	0.247	0.720	0.671	m
Sunflower	2.720	b	0.200	e	0.440	i	1.197	1.795	0.330	0.000	3.322	l	123	2.843	0.133	0.389	0.362	m
Sugar beet	9.540	b	0.126	e	0.467	i	4.459	0.245	0.245	0.164	5.114	l	56	9.516	0.446	1.301	1.212	m
Soybean	3.479	c	0.230	g	0.440	j	1.531	2.291	0.735	0.478	5.035	l	8	0.000	0.000	0.000	0.000	m
Miscanthus	22.788	d	0.126	f	0.475	j	10.835	12.218	12.995	4.332	40.379	l	52	1.505	0.071	0.206	0.192	m
Switchgrass	15.714	a	0.126	e	0.497	k	7.805	0.000	5.451	3.54	16.796	l	65	0.983	0.046	0.134	0.125	m
Cattle effluents	N/A		0.558	h	0.055	k	N/A	N/A	N/A	N/A	N/A		N/A	N/A	N/A	N/A	N/A	
Poultry effluents	N/A		0.308	h	0.154	k	N/A	N/A	N/A	N/A	N/A		N/A	N/A	N/A	N/A	N/A	
Swine effluents	N/A		0.462	h	0.083	k	N/A	N/A	N/A	N/A	N/A		N/A	N/A	N/A	N/A	N/A	
Other soil amendments (proxy compost)	N/A		0.670	h	0.130	k	N/A	N/A	N/A	N/A	N/A		N/A	N/A	N/A	N/A	N/A	

Sources: a (AGRESTE, 2019), b (Besnard et al., 2014), c (Cattelan and Dall’Agnol, 2018), d (Strullu et al., 2014), e (Duparque et al., 2013; Irizar et al., 2015; Moreno et al., 2016; Saffih-Hdadi and Mary, 2008), f (UNIFA, 1998), g (Irizar et al., 2015; Moreno et al., 2016), h (Agro-Transfert, 2019; Bouthier et al., 2014), i (PHYLLIS 2 database, 2019), j (Ma et al., 2018), k (Avadí, 2019), l (Bolinder et al., 2007; Carvalho et al., 2017; Richter et al., 2016; Strullu et al., 2014), for miscanthus aboveground inputs between 40% and 67% (Carvalho et al., 2017; Strullu et al., 2014) and perennial belowground proportions of rhizomes 75% and roots 25% (Agostini et al., 2015), m (AGRESTE, 2019, 2014, 2011; Avadí, 2019; FAO, 2004). “Effluents” refers to average values from manures, slurries and droppings (poultry). Modelling details of specific crops: maize (as a mean of grain and fodder), miscanthus (as permanent prairie), switchgrass (as temporary prairie), wheat (as a mean of hard and soft).

Descriptions of sub-indices: P - agricultural aboveground product, S - residual aboveground compartment, R - root/rhizome tissue, E - extra-root material.

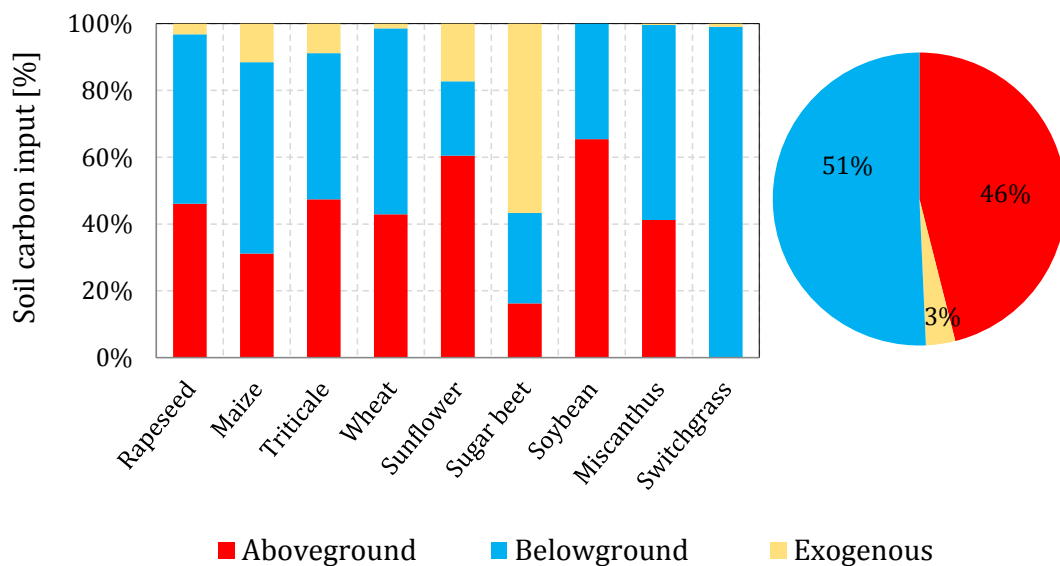
415

416 **3.3 Carbon inputs to the soil**

417 Fig. 3 shows the relative C added to the soil per energy crop in proportion to the AG and BG plant fractions, as
 418 well EX matter. The C inputs vary considerably among the different energy crop types, yet BG and AG have
 419 highest contributions to SOC, as compared with organic fertilisers.

420 In this study, the comparatively higher C contributions are associated with BG (Fig. 3), ranging (from smaller to
 421 higher) between 20% and 30% for sunflower and sugar beet, between 35% and 45% for soybean and triticale,
 422 between 50% and 60% for rapeseed, wheat, maize and miscanthus, and up to 100% for switchgrass.

423 Switchgrass has no residues (except for a disregarded minor amount of stubble), while the AG proportion of
 424 other crop types range between 16% and 31% for sugar beet and maize, between 40% and 50% for miscanthus,
 425 wheat, rapeseed and triticale, and the highest contribution from sunflower (60%) and soybean (65%). The
 426 remaining proportions associated with EX is rather low, yet with considerable differences per crop type,
 427 highest for sugar beet (57%), sunflower (17%), maize (12%) and triticale (9%). Note that the inputs are rather
 428 case- and site-specific, management practices may involve higher EX inputs due to displacement of inorganic
 429 fertilisers or higher/lower removal rates for AG/BG matter.



430 **■ Aboveground ■ Belowground ■ Exogenous**

431 Fig. 3. Soil carbon inputs per biomass commodity from above- and belowground plant compartments, including exogenous
 432 matter. Pie chart represents the average proportions

433

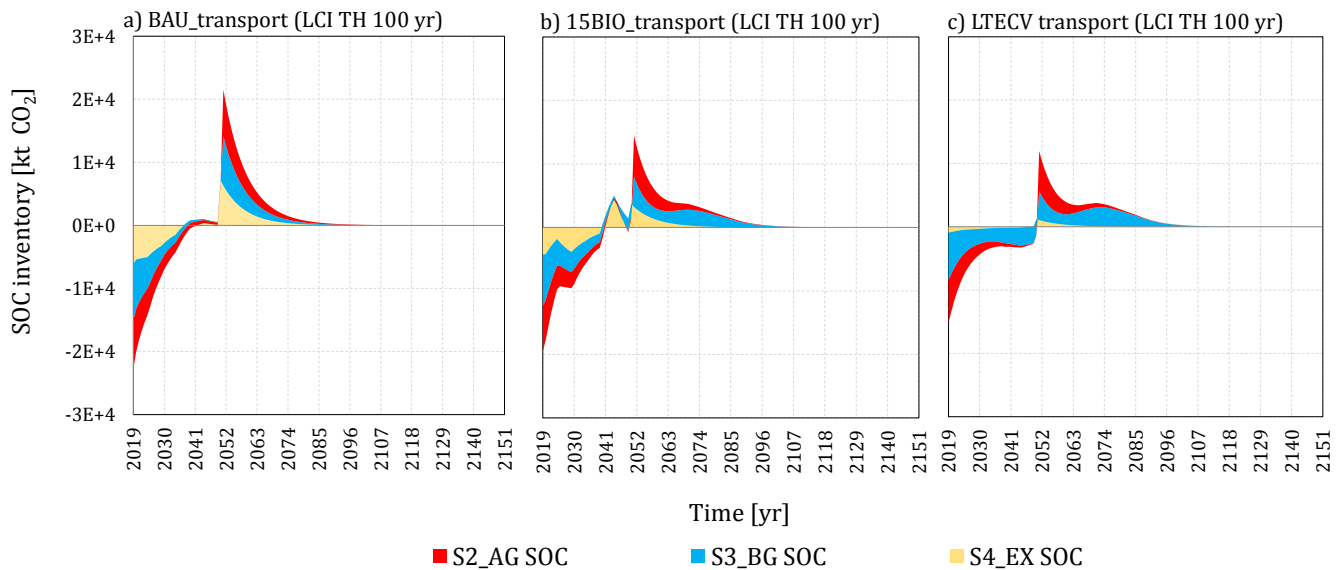
434 Fig. 4 shows the dynamic SOC inventories associated with policy and C input scenarios. It represents the
435 dynamic elementary flows resulting from the coupling with the PEM biomass commodity outputs (technical
436 flows) per policy scenario, i.e. BAU (Fig. 4a), 15BIO (Fig. 4b) and LTECV (Fig. 4c). The flows are expressed in t
437 CO₂ according to the C content in the compound (44/12 g CO₂.g⁻¹). Other GHG emissions from decay, such as
438 methane, are not accounted for, but should be considered in future studies.

439 The net annual SOC balance adds up all C inputs (negative values) per simulation year and the subsequent
440 gradual releases (positive values) from decay of all previous and consecutive years. The end-year 2050 shows
441 an “artificial cut-off” due to the ending of the prospective assessment of the PEM with no further biomass
442 mobilisation. Therefore, the year 2050 reveals peaking positive values.

443 For this study, the selected TH projects the last year of the PEM simulation period over an additional century,
444 that is to say from 2050 to 2150. The TH generally defines the length of time over which the GHG emissions are
445 integrated (Levasseur et al., 2016) (in static methods fixed to 20 or 100 years), however is flexible in dynamic
446 LCA (Levasseur et al., 2010) and can be adapted to any dynamic inventory TH, as discussed in (Albers et al.,
447 2019b). The determination of a TH remains subjective, as no theoretical foundation has been identified, but
448 only a political one (the widely accepted IPCC 100 years TH). The chosen TH over 100 years is valid here for the
449 SOC inventory flows as well as for the subsequent impact assessment. The temporal cut-off for SOC inventories
450 at year 2150 is justifiable: after the first century, the remaining SOC-sourced CO₂ range between 6E-5 and 4E-5,
451 assuming here at the given TH that an equivalent zero net C balance is reached (i.e. carbon neutrality). The first
452 SOC input in the year 2019 represents the highest SOC sequestration potential, decreasing with increasing
453 inventory time horizon (LCI TH).

454 A comparison among variations of TIMES-MIRET scenarios featuring the origin of different C inputs denotes a
455 particular SOC dynamic associated with S3_BG in 15BIO and LTECV. Note that S3_BG has a longer sequestration
456 curve and extended release flows, as compared with the S2_AG and S4_EX contributions. This phenomenon
457 relates with the perennial grasses introduced for advanced biofuels to respond to the new policy constraints.
458 This type of energy crop involves biomass growth and carbon fixation dynamic of rhizomes during the rotation

459 length. Moreover, the proportions of the AG and BG SOC flows (S2_AG and S3_BG) in the first inventory year
 460 2019, demonstrated that the two input variations contribute to SOC in similar proportions for BAU (32% and
 461 38%, 15BIO (36% and 41%) and LTECV (44% and 49%). In contrast, S4_EX considerably decreases for 15BIO
 462 (22%) and LTECV (7%) compared with BAU (29%). The cumulative sum of all C inputs (referring to S1_TOT)
 463 represented SOC contributions of about 40%, 34%, and 26% for BAU, 15BIO and LTECV scenarios respectively.



465 Fig. 4. Soil organic carbon inventories over a time horizon of 100 years [kt CO₂] per TIMES-MIRET (BAU, 15BIO, LTECV) and
 466 C input (S2_AG, S3_BG, S4_EX) scenarios

467 3.4 Dynamic impact assessment: Radiative forcing effects per policy and management scenario

468 Fig. 5 shows the instantaneous [in W·m⁻²] and cumulative [W·yr·m⁻²] radiative forcing (RF) effects per policy and
 469 C input scenarios over a 100-year LCIA TH. The 100-year reference is recommended by the IPCC guidelines
 470 (Myhre et al., 2013) and most commonly used in LCA, yet any future reference year could be chose with
 471 dynamic LCA (Levasseur et al., 2016, 2010). The RF effects are given for SOC (i.e. biogenic-sourced), C-neutral
 472 (i.e. fossil-sourced), as well as the C-complete (i.e. SOC + C-neutral). The overall results show considerable
 473 variations between C-neutral and C-complete effects, due to SOC accounting.

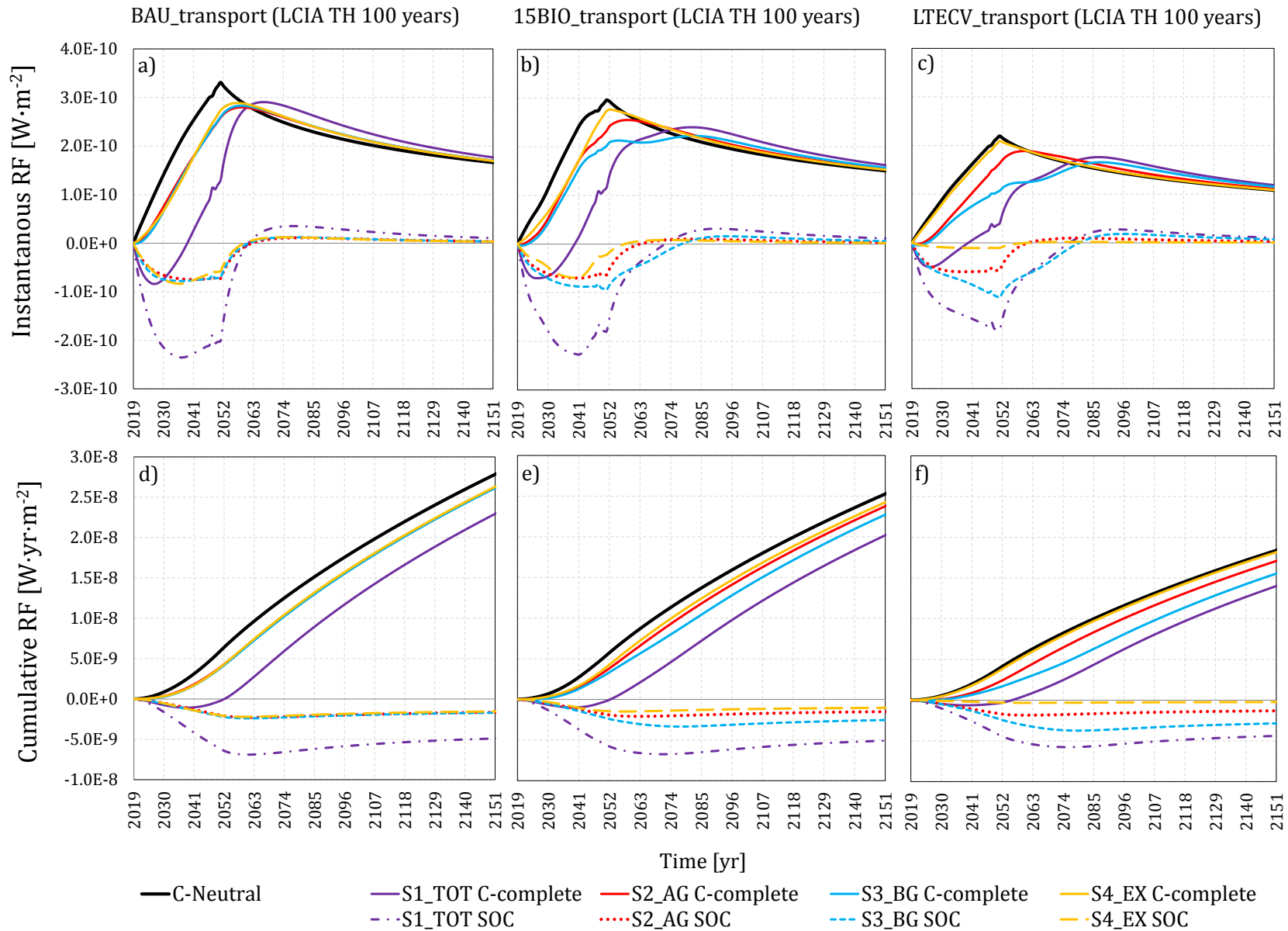
474 Instantaneous RF (Fig. 5a, b, and c) refers to the GHG concentrations and their induced net concentration
 475 change (Myhre et al., 2013). It allows describing the net changes through time. The “artificial cut-off” at year
 476 2050 is evident. For SOC emissions, it means that no further inputs are computed and therefore the positive

477 emissions outweigh the negative ones until equilibrium is reached and all emissions are returned back to the air
478 (referred here as a net zero C-balance). The annual cumulative RF effect (Fig. 5d, e, and f) of a pulse emission is
479 given by integrating the instantaneous forcing, allowing a direct comparison among scenarios. Firstly, it is
480 identifiable that the C-neutral effects are considerably lower for LTECV than for BAU and 15BIO. It reveals that
481 the constraints lead towards higher climate mitigation targets. Secondly, the annual negative effects from SOC-
482 CO₂ flows further reduce the C-neutral results in all analysed policy scenarios within the first century,
483 contributing to climate mitigation. The mitigation is higher for S3_BG (and consequently S1_TOT) in 15BIO (Fig.
484 5b) and LTECV (Fig. 5c).

485 A quantitative comparison of the cumulative RF of C-neutral and C-complete results per policy scenario can
486 only be undertaken by selecting an end-year of the impact assessment (reference year), here 2150. The C-
487 neutral results of 15BIO ($2.5E-8 \text{ W}\cdot\text{yr}\cdot\text{m}^{-2}$) and LTECV ($1.8E-8 \text{ W}\cdot\text{yr}\cdot\text{m}^{-2}$) show reduced forcing effects by about
488 10% and 34% respectively compared with the BAU reference ($2.8E-8 \text{ W}\cdot\text{yr}\cdot\text{m}^{-2}$). The accounting of SOC flows
489 further reduce the cumulative RF effects, as highlighted with C-complete results. S1_TOT (S2_AG + S3_BG +
490 S4_EX) represents the highest reduction potentials for 15BIO ($2E-8 \text{ W}\cdot\text{yr}\cdot\text{m}^{-2}$) and LTECV ($1.4E-8 \text{ W}\cdot\text{yr}\cdot\text{m}^{-2}$)
491 versus BAU ($2.5E8 \text{ W}\cdot\text{yr}\cdot\text{m}^{-2}$), whereof 50% and 65% are BG contributions given in 15BIO and LTECV scenarios
492 respectively (see also the Supplementary Material).

493 However, SOC benefits decrease with increasing LCIA TH, that is to say, the more into the future the reference
494 end-year is set, the lower are the contributions to climate mitigation. Firstly, this is due to the artificial cut-off
495 associated to the PEM analysis. Secondly, in the long-term (beyond a 100-year LCIA TH), all SOC-sourced CO₂
496 emissions converge to equilibrium, reaching a steady state, as all emissions return to the air. Yet, without the
497 consideration of SOC emissions, the negative RF (cooling effects), and thus the temporary climate benefits, are
498 not account for, leading to biased net C balance results over time.

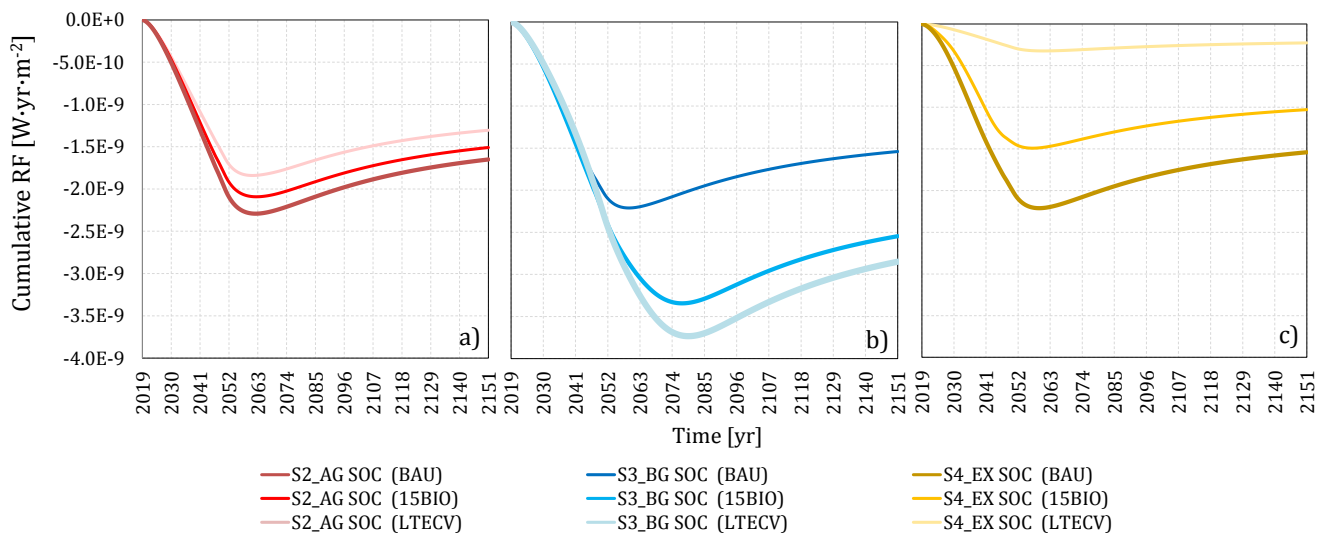
499



500

501 Fig. 5. Instantaneous [$W \cdot m^{-2}$] and cumulative [$W \cdot yr \cdot m^{-2}$] radiative forcing per policy (BAU, 15BIO and LTECV) and C input (S1_TOT, S2_AG, S3_BG, S4_EX) scenarios,
 502 denoting the dynamic impacts from biogenic- (here SOC flows) and fossil- (C neutral) sourced emissions, as well the sum of both in C-complete

503 The forcing contribution of the different SOC compartments become more evident by taking a closer look into
 504 the cumulative RF effect of AG (Fig. 6a), BG (Fig. 6b) and EX (Fig. 6c) per policy constraint. The highest
 505 contributions to climate mitigation are associated with S3_BG in both 15BIO and LTECV, reducing BAU by 150%
 506 and 170% respectively. This is due to biomass growth of rhizomes of perennial grasses that are not
 507 incorporated into the soil until the end of the rotation length, and thus represent temporal C-stock delaying
 508 degradation emissions. Consequently, the temporary sequestration and storage has climatic benefits due to
 509 postponement of positive RF (warming effects). The negative RF effects from perennial grasses and their
 510 derivative biofuels may represent a better alternative to annual crops in terms of climate change mitigation.



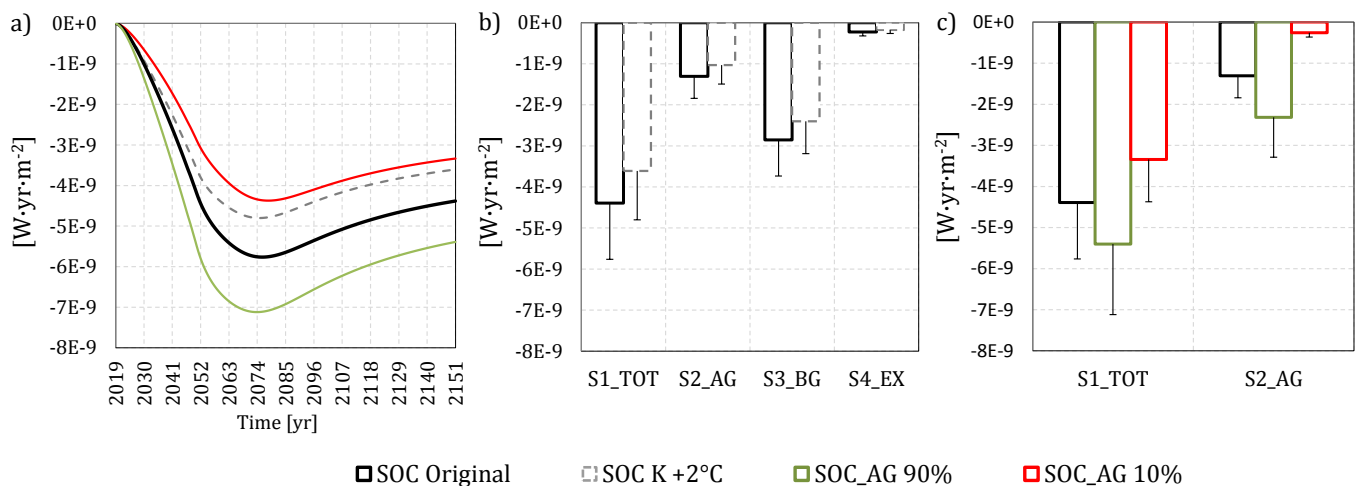
511
 512 Fig. 6. Cumulative radiative forcing [$\text{W}\cdot\text{yr}\cdot\text{m}^{-2}$] per policy (BAU, 15BIO and LTECV) and C input (S2_AG, S3_BG, S4_EX)
 513 scenarios

514 3.5 Sensitivity analysis

515 We conducted a sensitivity analysis for the LTECV policy scenario concerning i) the SOC model k coefficient
 516 (uncertainty due to site-dependent pedoclimatic conditions), and ii) the C inputs to the soil (variations in
 517 residue removal rates from the field). Therefore, k for type 3 pedoclimatic conditions were recalculated,
 518 assuming a temperature increase of 2°C (referred to as SOC $K+2^\circ\text{C}$) due to climate change, resulting in 0.1485,
 519 similar to k for oceanic climate type 5. k for SOC $K+2^\circ\text{C}$ in Brazil is 0.0924, yet soybean is excluded in the LTECV
 520 simulations. The removal rates concerned the S2_AG compartment (and consequently S1_TOT), for which we

521 run the SOC simulations, assuming two variations equally applied to all energy crops, namely 90% (referred to
 522 as SOC_AG 90%) and 10% (referred to as SOC_AG 10%) C input to the soil.

523 The cumulative RF results from 2019 to 2150 (in Fig. 7a), demonstrate significant variations between model
 524 parameter and C input to the soil. A quantitative comparison at year 2150 (in Fig. 7b) per C input scenario,
 525 shows a difference between the original values and SOC K+2°C results by 122%, 127%, 119% and 127% for
 526 S1_TOT, S2_AG, S3_BG, and S4_EX respectively. Two major interpretations are drawn. Firstly, SOC benefits
 527 decrease with increasing temperature (climate change), because the decay rate increases with temperature
 528 and thus C releases to the atmosphere occur over a shorter TH. Secondly, exogenous inputs (S4_EX) are more
 529 affected by temperature changes, because they already have high h values and thus lower initial SOC.
 530 Regarding the C input variations from SOC_AG residues at year 2150 (in Fig. 7c) S1_TOT original values increase
 531 with SOC_AG 90% (due to S2_AG benefit contribution by almost 60%) and decrease with SOC_AG 10% (due
 532 S2_AG deficit contributions by about 500%). Fig. 7b and c additionally show the minimum attainable values,
 533 representing the peak sequestration potential attributable to the year 2074 (Fig. 7a). This sensitivity is given
 534 due to the selected end-year 2150, which results in lower climatic benefits than the year 2074, linked with the
 535 artificial cut-off of the PEM simulation at year 2050.



537 Fig. 7. Cumulative radiative forcing [W·yr·m⁻²] from the sensitivity analysis results a) over the time horizon 2019 to 2119, b)
 538 quantitative uncertainty concerning k coefficient and temperature variations, and c) effect from changes in C inputs. b)
 539 and c) represent the year 2019 including uncertainty (error bar represent the minimum attainable value)

540

541 The variations of residue removal rates have significant consequences on the LU requirements (see Sensitivity
542 analysis on LU in the Supplementary Material). The residue removal rate for energy is an important
543 consideration, as it defines the equivalent agricultural area requirements to meet the energy demand of 2G
544 biofuels. SOC_AG 90% represent minimum and SOC_AG 10% maximum values in terms of residue export from
545 the fields and the inverse for C inputs to the soil. The higher the residue removal rate for energy the higher per
546 unit of area demand: for SOC_AG 10% (i.e. 90% removal rate) LU requirements increase by a factor of 5, while
547 for SOC_AG 90% (i.e. 10% removal rate) decrease by a factor of 0.56. Consequently, trade-off results for the
548 same unit of energy [MJ] produced between higher removals rates versus climate benefits from C inputs to the
549 soil. Note that other relevant factors (e.g. effects on biodiversity, N-mineralisation, yields) —not considered in
550 this study— may play an essential role.

551 **3.6 Limitations of the proposed approach**

552 The coupling framework is generic enough to be used in combination with any demand model or life cycle
553 inventory; however, other essential soil quality indicators and impacts from LUC are not included in the
554 proposed SOC modelling approach. The dynamic of these indicators (e.g. the set of indicators included in
555 LANCA) also needs to be developed to improve the results from soil activities modelling.

556 Furthermore, it is encouraged to use primary data when available to reduced uncertainties from averaged
557 values. The use of secondary data may compound the overall (data + model) uncertainty, yet it can in principle
558 be reduced by data processing and model calibration. Model calibration in particular, which implies the
559 selection of starting values, may nonetheless be biased, and thus self-starting models may be used to find
560 initial conditions for the main models, or, even better, observations data should be used if available.

561 Data processing should aim to improve the statistical representativeness and coherence of the data. The
562 presented SOC model could be replaced by or combined with alternative models with different structure, or
563 contrasted with other models, for ultimately more robust findings and lower uncertainty in predicting C
564 dynamics in the soil (Shi et al., 2018).

565 **4 Conclusions**

566 The overall comparison among the policy and C input scenarios to the soil shows achievable climate mitigation
567 targets in the transport sub-sector by means of shifting 1G-biomass share towards 2G (advanced) biofuels,
568 particularly given the LTECV policy. Dynamic SOC accounting makes a considerable difference in the C-complete
569 assessment. Without its modelling, temporary mitigation is ignored, thus biasing GHG emission results. Highest
570 mitigation contributions are attributed to perennial grasses, further delaying radiative forcing due to C
571 sequestration in the rhizomes fraction during the entire rotation length. Yet, cooling effects from SOC decrease
572 with increasing LCIA TH, as all emissions return to the atmospheric pool in the long-term. A sensitivity analysis
573 confirmed the SOC variability due to temperature (+2°C increase) and residue removal rates changes. Both
574 affect climate mitigation and the latter also LU by a factor of -0.56 to +5. In the context of LCA, the
575 consideration of other direct and indirect impacts associated with changes in LU, management (e.g. tillage and
576 land preparation, fertiliser use, crop and yield protection, erosion measures) and LUC, including biodiversity
577 should follow suit to better understand trade-offs.

578 **5 Acknowledgements**

579 The authors would like to acknowledge the support by IFP Energies nouvelles, division of Economics &
580 Technology Intelligence. This work was financed by a doctoral grant as part of the Ph.D. research project.
581 Moreover, the authors are grateful for the useful comments provided by the Reviewers.

582 **References**

- 583 ADEME, 2017. Mobilisation de la Biomasse Agricole : état de l'art et analyse prospective. ADEME, Deloitte Développement
584 Durable, Association d'Initiatives Locales pour l'Energie et l'Environnement (AILE), Alterra Wageningen. Angers.
585 France.
- 586 Agostini, F., Gregory, A.S., Richter, G.M., 2015. Carbon Sequestration by Perennial Energy Crops : Is the Jury Still Out ?
587 Bioenergy Res. 1057–1080. <https://doi.org/10.1007/s12155-014-9571-0>
- 588 AGRESTE, 2019. Agreste - Données en ligne [WWW Document]. Ministère de l'Agriculture et de l'Alimentation. URL
589 <https://stats.agriculture.gouv.fr/disar-web/disaron/!searchurl/searchUuid/search.disar> (accessed 2.1.19).
- 590 AGRESTE, 2014. Enquête sur les pratiques culturales 2011: Principaux résultats, Ministère de l'Agriculture, de

591 l'Agroalimentaire et de la Forêt. Agreste les Dossiers No. 21. Montreuil Sous Bois Cedex, France.

592 AGRESTE, 2011. Statistique Agricole Annuelle 2010 No 25, Direction Régionale de l'Alimentation de l'Agriculture et de la
593 Forêt. Service Régional de l'Information Statistique et Economique. Rennes Cedex, France.

594 Agro-Transfert, 2019. SIMEOS-AMG -Guide Utilisateur: Gérer l'état organique du sol dans les exploitations agricoles. Agro-
595 Transfert Ressources et Territoires, INRA, Arvalis et Terres Inovia. France.

596 Albers, A., Collet, P., Benoist, A., Hélias, A., 2019a. Back to the future : Dynamic full carbon accounting applied to
597 prospective bioenergy scenarios. *Int. J. Life Cycle Assess.* 1-27]. <https://doi.org/DOI: 10.1007/s11367-019-01695-7>

598 Albers, A., Collet, P., Lorne, D., Benoist, A., Hélias, A., 2019b. Coupling partial-equilibrium and dynamic biogenic carbon
599 models to assess future transport scenarios in France. *Appl. Energy* 239, 316–330.
600 <https://doi.org/10.1016/j.apenergy.2019.01.186>

601 Andren, O., Kätterer, T., 1997. ICBM: The introductory carbon balance model for exploration of soil carbon balances. *Ecol.*
602 *Appl.* 7, 1226–1236. <https://doi.org/10.2307/2641210>

603 Andriulo, A., Mary, B., Guerif, J., Andriulo, A., Mary, B., Guerif, J., Andriulo, A., 1999. Modelling soil carbon dynamics with
604 various cropping sequences on the rolling pampas. *Agron. EDP Sci.* 19, 365–377.

605 Arevalo, C.B.M., Bhatti, J.S., Chang, S.X., Sidders, D., 2011. Agriculture , Ecosystems and Environment Land use change
606 effects on ecosystem carbon balance : From agricultural to hybrid poplar plantation. "Agriculture, Ecosyst. Environ."
607 141, 342–349. <https://doi.org/10.1016/j.agee.2011.03.013>

608 Avadí, A., 2019. Screening LCA of French organic amendments and fertilisers. *Int. J. Life Cycle Assess.* [under Rev.].

609 Beck, T., Bos, U., Wittstock, B., Baitz, M., Fischer, M., Sedlbauer, K., 2010. LANCA- Land Use Indicator Value Calculation in
610 Life Cycle Assessment – Method Report. Fraunhofer Institute for Building Physics and University of Stuttgart.
611 Echterding.

612 Benbi, D.K., Richter, J., 2002. A critical review of some approaches to modelling nitrogen mineralization. *Biol. Fertil. Soils*
613 35, 168–183. <https://doi.org/10.1007/s00374-002-0456-6>

614 Benoist, A., Bessou, C., 2018. Prise en compte en Analyse de Cycle de Vie (ACV) du lien usage des sols – changement
615 climatique : revue critique des methodologies existantes. *Proj. SOCLE, soil Org. carbon Chang. LCA, which Eval. to*
616 *Improv. Environ. assessments?* 1–101.

617 Benoist, A., Cornillier, C., 2016. Towards a consensual method to assess climate change impacts from bio-based systems,
618 in: SETAC Europe Annual Meeting: Environmental Contaminants from Land to Sea: Continuities and Interface in
619 Environmental Toxicology and Chemistry. Nantes : SETAC Europe, 2 p. SETAC Europe Annual Meeting: Environmental
620 Contaminants from Land to Sea: Continuit.

621 Besnard, A., Ferchaud, F., Levraut, F., Nguyen, E., Marsac, S., Savouré, M., 1, 2014. Le Lignoguide: Une aide aux choix des
622 cultures biomasse. *Innov. Agron.* 34, 35–50.

623 Beuch, S., Boelcke, B., Belau, L., 2000. Effect of the organic residues of *Miscanthus x giganteus* on the soil organic matter
624 level of arable soils. *J. Agron. Crop Sci.* 184, 111–119. <https://doi.org/10.1046/j.1439-037X.2000.00367.x>

625 Bockstaller, C., Girardin, P., 2010. Mode de calcul des indicateurs agri-environnementaux de la methode Indigo®, UMR
626 INPL(ENSAIA)-INRA Agronomie et Environnement. Nancy-Colmar BP. France.

627 Bolinder, M.A., Janzen, H.H., Gregorich, E.G., Angers, D.A., VandenBygaart, A.J., 2007. An approach for estimating net
628 primary productivity and annual carbon inputs to soil for common agricultural crops in Canada. *Agric. Ecosyst.*
629 *Environ.* 118, 29–42. <https://doi.org/10.1016/j.agee.2006.05.013>

630 Bolinder, M.A., Vandenbygaart, A.J., Gregorich, E.G., Angers, D.A., Janzen, H.H., 2006. Modelling soil organic carbon stock
631 change for estimating whole-farm greenhouse gas emissions. *Can. J. Soil Sci.* 86, 419–429.
632 <https://doi.org/10.4141/S05-102>

633 Bos, U., Horn, R., Beck, T., Lindner, J.P., Fischer, M., 2016. LANCA® Characterization Factors for Life Cycle Impact
634 Assessment. Version 2.0. Fraunhofer Institute for Building Physics. Fraunhofer Verlag. Stuttgart. Germany.

635 Bouthier, A., Duparque, A., Mary, B., Sagot, S., Trochard, R., Levert, M., Houot, S., Damay, N., Denoroy, P., Dinh, J.-L., Blin,
636 B., Ganteil, F., 2014. Adaptation et mise en œuvre du modèle de calcul de bilan humique à long terme AMG dans
637 une large gamme de systèmes de grandes cultures et de polyculture-élevage. *Innov. Agron.* 34, 125–139.

638 Brandão, M., Lévassieur, A., Kirschbaum, M.U.F., Weidema, B.P., Cowie, A.L., Jørgensen, S.V., Hauschild, M.Z., Pennington,
639 D.W., Chomkamsri, K., 2013. Key issues and options in accounting for carbon sequestration and temporary storage
640 in life cycle assessment and carbon footprinting. *Int. J. Life Cycle Assess.* 18, 230–240.

641 <https://doi.org/10.1007/s11367-012-0451-6>

642 Brandão, M., Milà i Canals, L., 2013. Global characterisation factors to assess land use impacts on biotic production. *Int. J.*
643 *Life Cycle Assess.* 18, 1243–1252. <https://doi.org/10.1007/s11367-012-0381-3>

644 Brandão, M., Milà i Canals, L., Clift, R., 2011. Soil organic carbon changes in the cultivation of energy crops: Implications for
645 GHG balances and soil quality for use in LCA. *Biomass and Bioenergy* 35, 2323–2336.
646 <https://doi.org/10.1016/j.biombioe.2009.10.019>

647 Brilli, L., Bechini, L., Bindi, M., Carozzi, M., Cavalli, D., Conant, R., Dorich, C.D., Doro, L., Ehrhardt, F., Farina, R., Ferrise, R.,
648 Fitton, N., Francaviglia, R., Grace, P., Iocola, I., Klumpp, K., Léonard, J., Martin, R., Massad, R.S., Recous, S., Seddaiu,
649 G., Sharp, J., Smith, P., Smith, W.N., Soussana, J.F., Bellocchi, G., 2017. Review and analysis of strengths and
650 weaknesses of agro-ecosystem models for simulating C and N fluxes. *Sci. Total Environ.* 598, 445–470.
651 <https://doi.org/10.1016/j.scitotenv.2017.03.208>

652 BSI, 2011. PAS 2050:2011 - Specification for the assessment of the life cycle greenhouse gas emissions of goods and
653 services, BSI 2011. London: The British Standards Institution. <https://doi.org/978 0 580 71382 8>

654 Caldeira-Pires, A., Benoist, A., Luz, S.M. da, Silverio, V.C., Silveira, C.M., Machado, F.S., 2018. Implications of removing
655 straw from soil for bioenergy: An LCA of ethanol production using total sugarcane biomass. *J. Clean. Prod.* 181, 249–
656 259. <https://doi.org/10.1016/j.jclepro.2018.01.119>

657 Campbell, E.E., Paustian, K., 2015. Current developments in soil organic matter modeling and the expansion of model
658 applications: A review. *Environ. Res. Lett.* 10. <https://doi.org/10.1088/1748-9326/10/12/123004>

659 Campell, E., Paustian, K., 2015. Current developments in soil organic matter modeling and the expansion of model
660 applications. *Environ. Res. Lett.* 10, 123004. <https://doi.org/10.1088/1748-9326/10/12/123004>

661 Carvalho, J.L., Hudiburg, T.W., Franco, H.C., DeLucia, E.H., 2017. Contribution of above- and belowground bioenergy crop
662 residues to soil carbon. *GCB Bioenergy* 9, 1333–1343. <https://doi.org/10.1111/gcbb.12411>

663 Cattelan, A.J., Dall’Agnol, A., 2018. The rapid soybean growth in Brazil. *Oilseeds fats Crop. Lipids* 25, D102.
664 <https://doi.org/10.1051/ocl/2017058>

665 CGIAR, 2018. 4 pour 1000: Preserving soils for carbon capture and food security [WWW Document]. *Res. Progr. Water, L.*
666 *Ecosyst.* URL <https://wle.cgiar.org/4-pour-1000-preserving-soils-carbon-capture-and-food-security> (accessed 2.1.18).

667 Ci, E., Al-kaisi, M.M., Wang, L., Ding, C., Xie, D., 2015. Soil Organic Carbon Mineralization as Affected by Cyclical
668 Temperature Fluctuations in a Karst Region of Southwestern China. *Pedosphere* 25, 512–523.
669 [https://doi.org/10.1016/S1002-0160\(15\)30032-1](https://doi.org/10.1016/S1002-0160(15)30032-1)

670 Clivot, H., Mouny, J.-C., Duparque, A., Dinh, J.-L., Denoroy, P., Houot, S., Vertès, F., Trochard, R., Bouthier, A., Sagot, S.,
671 Mary, B., 2019. Modeling soil organic carbon evolution in long-term arable experiments with AMG model. *Environ.*
672 *Model. Softw.* 118, 99–113. <https://doi.org/10.1016/j.envsoft.2019.04.004>

673 Coleman, K., Jenkinson, D.S., 2014. RothC - A model for the turnover of carbon in soil. Model description and users guide
674 (updated June 2014), Rothamsted Research. Rothamsted Research. Herts, UK.

675 Delphin, J.E., 2000. Estimation of nitrogen mineralization in the field from an incubation test and from soil analysis.
676 *Agronomie* 20, 349–361. <https://doi.org/10.1051/agro:2000132>

677 Duparque, A., Dinh, J., Mary, B., Bouthier, A., Blin, B., Denoroy, P., Ganteil, F., Houot, S., Levert, M., Sagot, S., Trochard, R.,
678 Territoires, A.R., Brunehaut, C., 2013. AMG : a simple SOC balance model used in France for decision support, in:
679 SOMpatic (November 20-22, 2013). Rauschholtzhausern. Germany.

680 Dupuy, L., Gregory, P.J., Bengough, A.G., 2010. Root growth models: Towards a new generation of continuous approaches.
681 *J. Exp. Bot.* 61, 2131–2143. <https://doi.org/10.1093/jxb/erp389>

682 EC-JRC, 2010. Framework and Requirements for Life Cycle Impact Assessment Models and Indicators, International
683 Reference Life Cycle Data System (ILCD) Handbook. European Commission - Joint Research Centre - Institute for
684 Environment and Sustainability. <https://doi.org/10.2788/38719>

685 EC, 2018a. EU Climate Action: Climate strategies & targets [WWW Document]. *Eur. Comm. Platf.* URL
686 https://ec.europa.eu/clima/policies/strategies_en (accessed 2.7.18).

687 EC, 2018b. Product Environmental Footprint Category Rules Guidance v6.3, PEFCR Guidance document, - Guidance for the
688 development of Product Environmental Footprint Category Rules (PEFCRs), version 6.3. Ispra: JRC-Joint Research
689 Centre, Italy.

690 Edwards, R., Lariv’, J.-F., Richeard, D., Weinhof, W., 2014. Well-to-Tank Report” Version 4.a: JEC Well-To-Wheels Analysis

691 of Future Automotive Fuels and Powertrains in the European Context, Report EUR 26237 EN. Ispra: JRC-Joint
692 Research Centre. <https://doi.org/10.2790/95629>

693 Eurostat, 2019. Climate change - driving forces [WWW Document]. Web page Eurostat. URL
694 [https://ec.europa.eu/eurostat/statistics-](https://ec.europa.eu/eurostat/statistics-explained/index.php?title=File:Greenhouse_gas_emissions_by_IPCC_source_sector,_EU28,_change_from_1990_to_2016_(million_tonnes_of_CO2_equivalent_and_%25_change).png)
695 [explained/index.php?title=File:Greenhouse_gas_emissions_by_IPCC_source_sector,_EU28,_change_from_1990_to_](https://ec.europa.eu/eurostat/statistics-explained/index.php?title=File:Greenhouse_gas_emissions_by_IPCC_source_sector,_EU28,_change_from_1990_to_2016_(million_tonnes_of_CO2_equivalent_and_%25_change).png)
696 [2016_\(million_tonnes_of_CO2_equivalent_and_%25_change\).png](https://ec.europa.eu/eurostat/statistics-explained/index.php?title=File:Greenhouse_gas_emissions_by_IPCC_source_sector,_EU28,_change_from_1990_to_2016_(million_tonnes_of_CO2_equivalent_and_%25_change).png) (accessed 3.1.19).

697 FAO, 2018. Measuring and modelling soil carbon stocks and stock changes in livestock production systems: Guidelines for
698 assessment (Draft for public review), FAO publications. Livestock Environmental Assessment and Performance
699 (LEAP) Partnership. Rome, Italy.

700 FAO, 2017. Soil Organic Carbon: the hidden potential. Rome: Food and Agriculture Organization of the United Nations.

701 FAO, 2004. Fertilizer Use by Crop in Brazil Land and Plant Nutrition Management Service Land and Water Development
702 Division. FAO- Food and Agriculture Organisation of the United Nations. Rome.

703 Frank, S., Schmid, E., Havlík, P., Schneider, U.A., Böttcher, H., Balkovič, J., Obersteiner, M., 2015. The dynamic soil organic
704 carbon mitigation potential of European cropland. *Glob. Environ. Chang.* 35, 269–278.
705 <https://doi.org/10.1016/j.gloenvcha.2015.08.004>

706 Frisque, M., 2007. Gestion des matières organiques dans les sols cultivés en Région wallonne : avantages agronomiques,
707 avantages environnementaux et séquestration du carbone Directeurs. Université Libre de Bruxelles IGEAT Institut de
708 Gestion de l'Environnement et d'Aménagement du Territoire.

709 Gobin, A., Campling, L., Janssen, N., Desmet, H., Delden, V., Hurkens, J., Lavelle, P., Berman, S., 2011. Soil organic matter
710 management across the EU – best practices, constraints and trade-offs, Final Report for the European Commission's
711 DG Environment. Technical Report - 2011 - 051. <https://doi.org/10.2779/17252>

712 Goglio, P., Grant, B.B., Smith, W.N., Desjardins, R.L., Worth, D.E., Zentner, R., Malhi, S.S., 2014. Impact of management
713 strategies on the global warming potential at the cropping system level. *Sci. Total Environ.* 490, 921–933.
714 <https://doi.org/10.1016/j.scitotenv.2014.05.070>

715 Goglio, P., Smith, W.N., Grant, B.B., Desjardins, R.L., Gao, X., Hanis, K., Tenuta, M., Campbell, C.A., McConkey, B.G.,
716 Nemecek, T., Burgess, P.J., Williams, A.G., 2018. A comparison of methods to quantify greenhouse gas emissions of
717 cropping systems in LCA. *J. Clean. Prod.* 172, 4010–4017. <https://doi.org/10.1016/j.jclepro.2017.03.133>

718 Goglio, P., Smith, W.N., Grant, B.B., Desjardins, R.L., McConkey, B.G., Campbell, C.A., Nemecek, T., 2015. Accounting for
719 soil carbon changes in agricultural life cycle assessment (LCA): A review. *J. Clean. Prod.* 104, 23–39.
720 <https://doi.org/10.1016/j.jclepro.2015.05.040>

721 Grogan P., Matthews, R., 2002. A modelling analysis of the potential for soil carbon sequestration under short rotation
722 coppice willow bioenergy plantations. *Soil Use Manag.* 18, 175–183. <https://doi.org/10.1079/SUM2002119>

723 Guest, G., Cherubini, F., Strømman, A.H., 2013. The role of forest residues in the accounting for the global warming
724 potential of bioenergy. *GCB Bioenergy* 5. <https://doi.org/10.1111/gcbb.12014>

725 Gueudet, A., 2012. Action CASDAR « ACV et fertilisation » Fiches sur les modèles d'émission. ACTA, ARVALIS, IRSTEA.

726 Han, X., Gao, G., Chang, R., Li, Z., Ma, Y., Wang, S., Wang, C., Lü, Y., Fu, B., 2018. Changes in soil organic and inorganic
727 carbon stocks in deep profiles following cropland abandonment along a precipitation gradient across the Loess
728 Plateau of China. *Agric. Ecosyst. Environ.* 258, 1–13. <https://doi.org/10.1016/j.agee.2018.02.006>

729 Harvey, M., Pilgrim, S., 2011. The new competition for land: Food, energy, and climate change. *Food Policy* 36, S40–S51.
730 <https://doi.org/10.1016/j.foodpol.2010.11.009>

731 Henin, S., Dupuis, M., 1945. Essai de bilan de la matière organique du sol. *Ann. Agron.* 1, 19–29.

732 Horn, R., Maier, S., 2018. LANCA®- Characterization Factors for Life Cycle Impact Assessment, Version 2.5. [WWW
733 Document]. Fraunhofer Inst. URL <http://publica.fraunhofer.de/documents/N-379310.html> (accessed 7.31.19).

734 INRA, 2019. Stocker du carbone dans les sols français : quel potentiel au regard de l'objectif 4 pour 1000 et à quel cout ?
735 Réalisée pour l'ADEME et le Ministère de l'Agriculture et de l'Alimentation. Paris.

736 IPCC, 2006. 2006 IPCC Guidelines for National Greenhouse Gas Inventories. The Intergovernmental Panel on Climate
737 Change (IPCC).

738 Irizar, A.B., Delaye, L.A.M., Andriulo, A.E., 2015. Projection of Soil Organic Carbon Reserves in the Argentine Rolling Pampa
739 Under Different Agronomic Scenarios. Relationship of these Reserves with Some Soil Properties. *Open Agric. J.* 9,
740 30–41. <https://doi.org/10.2174/1874331501509010030>

- 741 Joly, D., Brossard, T., Cardot, H., Cavailhes, J., Hilal, M., Wavresky, P., 2010. Les types de climats en France, une
742 construction spatiale - Types of climates on continental France, a spatial construction. *Cybergéo Eur. J. Geogr.* 1–23.
743 <https://doi.org/10.4000/cybergegeo.23155>
- 744 Koellner, T., Baan, L., Beck, T., Brandão, M., Civit, B., Margni, M., Canals, L.M., Saad, R., Souza, D.M., Müller-Wenk, R.,
745 2013. UNEP-SETAC guideline on global land use impact assessment on biodiversity and ecosystem services in LCA.
746 *Int. J. Life Cycle Assess.* 18, 1188–1202. <https://doi.org/10.1007/s11367-013-0579-z>
- 747 Kwiatkowska-Malina, J., 2018. Qualitative and quantitative soil organic matter estimation for sustainable soil
748 management. *J. Soils Sediments* 18, 2801–2812. <https://doi.org/10.1007/s11368-017-1891-1>
- 749 Le Villio, M., Arrouays, D., Deslais, W., Daroussin, J., Le Bissonnais, Y., Clergeot, D., 2001. Estimation des quantités de
750 matière organique exogène nécessaires pour restaurer et entretenir les sols limoneux français à un niveau
751 organique donné. *Etude Gest. des Sols* 8, 47–64.
- 752 Lehmann, J., Kleber, M., 2015. The contentious nature of soil organic matter. *Nature* 1–9.
753 <https://doi.org/10.1038/nature16069>
- 754 Lemus, R., Lal, R., 2005. Bioenergy crops and carbon sequestration. *CRC. Crit. Rev. Plant Sci.* 24, 1–21.
755 <https://doi.org/10.1080/07352680590910393>
- 756 Levasseur, A., Cavalett, O., Fuglestvedt, J.S., Gasser, T., Johansson, D.J.A., Jørgensen, S. V., Raugei, M., Reisinger, A.,
757 Schivley, G., Strømman, A., Tanaka, K., Cherubini, F., 2016. Enhancing life cycle impact assessment from climate
758 science: Review of recent findings and recommendations for application to LCA. *Ecol. Indic.* 71, 163–174.
759 <https://doi.org/10.1016/j.ecolind.2016.06.049>
- 760 Levasseur, A., Lesage, P., Margni, M., Deschênes, L., Samson, R., 2010. Considering time in LCA: Dynamic LCA and its
761 application to global warming impact assessments. *Environ. Sci. Technol.* 44, 3169–3174.
762 <https://doi.org/10.1021/es9030003>
- 763 Liang, B.C., Campbell, C.A., McConkey, B.G., Padbury, G., Collas, P., 2005. An empirical model for-estimating carbon
764 sequestration on the Canadian prairies. *Can. J. Soil Sci.* 85, 549–556. <https://doi.org/10.4141/S04-089>
- 765 Lorne, D., Tchung-Ming, S., 2012. The French biofuels mandates under cost uncertainty – an assessment based on robust
766 optimization. *Les Cah. l'économie* 33.
- 767 Loulou, R., Lehtilä, A., Kanudia, A., Remme, U., Goldstein, G., 2016. Documentation for the TIMES Model PART II:
768 Reference Manual, Energy Technology Systems Analysis Programme. ETSAP-Energy Technology Systems Analysis
769 Programme.
- 770 Luo, Y., Ahlström, A., Allison, S.D., Batjes, N.H., Brovkin, V., Carvalhais, N., Chappell, A., Ciais, P., Davidson, E.A., Finzi, A.,
771 Georgiou, K., Guenet, B., Hararuk, O., Harden, J.W., He, Y., Hopkins, F., Jiang, L., Koven, C., Jackson, R.B., Jones, C.D.,
772 Lara, M.J., Liang, J., McGuire, A.D., Parton, W., Peng, C., Randerson, J.T., Salazar, A., Sierra, C.A., Smith, M.J., Tian, H.,
773 Todd-brown, K.E.O., Torn, M., Groenigen, K.J., Wang, Y.P., West, T.O., Wei, Y., Wieder, W.R., Xia, J., Xu, Xia, Xu,
774 Xiaofeng, Zhou, T., 2016. Toward more realistic projections of soil carbon dynamics by Earth system models. *Global
775 Biogeochem. Cycles* 40–56. <https://doi.org/10.1002/2015GB005239>.Received
- 776 Ma, S., He, F., Tian, D., Zou, D., Yan, Z., Yang, Y., Zhou, T., Huang, K., Shen, H., Fang, J., 2018. Variations and determinants
777 of carbon content in plants: A global synthesis. *Biogeosciences* 15, 693–702. [https://doi.org/10.5194/bg-15-693-
778 2018](https://doi.org/10.5194/bg-15-693-2018)
- 779 Mi, J., Liu, W., Yang, W., Yan, J., Li, J., Sang, T., 2014. Carbon sequestration by *Miscanthus* energy crops plantations in a
780 broad range semi-arid marginal land in China. *Sci. Total Environ.* 496, 373–380.
781 <https://doi.org/10.1016/j.scitotenv.2014.07.047>
- 782 Milà i Canals, L., Bauer, C., Depestele, J., Dubreuil, A., Knuchel, R.F., 2007a. Key Elements in a Framework for Land Use
783 Impact Assessment Within LCA. *Int. J. Life Cycle Assess.* 12, 5–15. <https://doi.org/10.1065/lca2006.05.250>
- 784 Milà i Canals, L., Romanyà, J., Cowell, S.J., 2007b. Method for assessing impacts on life support functions (LSF) related to
785 the use of “fertile land” in Life Cycle Assessment (LCA). *J. Clean. Prod.* 15, 1426–1440.
786 <https://doi.org/10.1016/j.jclepro.2006.05.005>
- 787 Minasny, B., Malone, B.P., McBratney, A.B., Angers, D.A., Arrouays, D., Chambers, A., Chaplot, V., Chen, Z.-S., Cheng, K.,
788 Das, B.S., Field, D.J., Gimona, A., Hedley, C.B., Hong, S.Y., Mandal, B., Marchant, B.P., Martin, M., McConkey, B.G.,
789 Mulder, V.L., O'Rourke, S., Richer-de-Forges, A.C., Odeh, I., Padarian, J., Paustian, K., Pan, G., Poggio, L., Savin, I.,
790 Stolbovoy, V., Stockmann, U., Sulaeman, Y., Tsui, C.-C., Vågen, T.-G., van Wesemael, B., Winowiecki, L., 2017. Soil
791 carbon 4 per mille. *Geoderma* 292, 59–86. <https://doi.org/10.1016/j.geoderma.2017.01.002>

- 792 Moreno, R., Studdert, G.A., G, M.M., I, I.A., 2016. Soil organic carbon changes simulated with the AMG model in a high-
793 organic-matter Mollisol. *Spanish J. Soil Sci.* 6, 212–229. <https://doi.org/10.3232/SJSS.2016.V6.N3.04>
- 794 MTES, 2018. Loi de transition énergétique pour la croissance verte [WWW Document]. Ministère la Transit. écologique
795 solidaire. URL <https://www.ecologique-solidaire.gouv.fr/loi-transition-energetique-croissance-verte> (accessed
796 1.29.18).
- 797 Müller-Wenk, R., Brandão, M., 2010. Climatic impact of land use in LCA-carbon transfers between vegetation/soil and air.
798 *Int. J. Life Cycle Assess.* 15, 172–182. <https://doi.org/10.1007/s11367-009-0144-y>
- 799 Myhre, G., Shindell, D., Bréon, F.-M., Collins, W., Fuglestvedt, J., Huang, J., Koch, D., Lamarque, J.-F., Lee, D., Mendoza, B.,
800 Nakajima, T., Robock, A., Stephens, G., Takemura, T., Zhang, H., 2013. Chapter 8 Anthropogenic and Natural
801 Radiative Forcing, in: Stocker, T.F., D. Qin, G.-K. Plattner, M. Tignor, S.K. Allen, J. Boschung, A. Nauels, Y. Xia, V.B. and
802 P.M.M. (eds.). (Ed.), In: *Climate Change 2013: The Physical Science Basis. Contribution of Working Group I to the*
803 *Fifth Assessment Report of the Intergovernmental Panel on Climate Change* [Stocker, T.F., D. Qin, G.-K. Plattner, M.
804 Tignor, S.K. Allen, J. Boschung, A. Nauels, Y. Cambridge University Press, Cambridge, United Kingdom and New York,
805 pp. 659–740. <https://doi.org/10.1017/CBO9781107415324.018>
- 806 Nagy, R.C., Porder, S., Brando, P., Davidson, E.A., Figueira, A.M. e. S., Neill, C., Riskin, S., Trumbore, S., 2018. Soil Carbon
807 Dynamics in Soybean Cropland and Forests in Mato Grosso, Brazil. *J. Geophys. Res. Biogeosciences* 123, 18–31.
808 <https://doi.org/10.1002/2017JG004269>
- 809 Nemecek, T., Dubois, D., Huguenin-Elie, O., Gaillard, G., 2011. Life cycle assessment of Swiss farming systems: I. Integrated
810 and organic farming. *Agric. Syst.* 104, 217–232. <https://doi.org/10.1016/j.agsy.2010.10.002>
- 811 Nemecek, T., Kagi, T., 2007. Life Cycle Inventories of Agricultural Production Systems Data v2.0 (2007),ecoinvent report
812 No. 15. Swiss Center For Life Cycle Inventories.
- 813 Nicolardot, B., Recous, S., Mary, B., 2001. Simulation of C and N mineralisation during crop residue decomposition : A
814 simple dynamic model based on the C : N ratio of the residues 83–103. <https://doi.org/10.1023/A:1004813801728>
- 815 Oberholzer, H.-R., Knuchel, R.F., Weisskopf, P., Gaillard, G., 2012. A novel method for soil quality in life cycle assessment
816 using several soil indicators. <https://doi.org/10.1007/s13593-011-0072-7>
- 817 Oberholzer, H.-R., Weisskopf, P., Gaillard, G., Weiss, F., Freiermuth Knuchel, R., 2006. Methode zur Beurteilung der
818 Wirkungen landwirtschaftlicher Bewirtschaftung auf die Bodenqualität in Ökobilanzen.
- 819 Petersen, B.M., 2003. C-TOOL version 1.1. A tool for simulation of soil carbon turnover. Description and users guide.
820 Danish Institute of Agricultural Sciences.
- 821 Petersen, B.M., Knudsen, M.T., Hermansen, J.E., Halberg, N., 2013. An approach to include soil carbon changes in life cycle
822 assessments. *J. Clean. Prod.* 52, 217–224. <https://doi.org/10.1016/j.jclepro.2013.03.007>
- 823 PHYLLIS 2 database, 2019. Phyllis2: Database for biomass and waste [WWW Document]. ECN.TNO. URL <https://phyllis.nl/>
824 (accessed 2.20.19).
- 825 Rehbein, K., Sandhage-hofmann, A., Amelung, W., 2015. Soil carbon accrual in particle-size fractions under *Miscanthus x*
826 *giganteus* cultivation. *Biomass and Bioenergy* 78, 80–91. <https://doi.org/10.1016/j.biombioe.2015.04.006>
- 827 Richter, G.M., Agostini, F., Barker, A., Costomiris, D., Qi, A., 2016. Assessing on-farm productivity of *Miscanthus* crops by
828 combining soil mapping, yield modelling and remote sensing. *Biomass and Bioenergy* 85, 252–261.
829 <https://doi.org/10.1016/j.biombioe.2015.12.024>
- 830 Saffih-Hdadi, K., Mary, B., 2008. Modeling consequences of straw residues export on soil organic carbon. *Soil Biol.*
831 *Biochem.* 40, 594–607. <https://doi.org/10.1016/j.soilbio.2007.08.022>
- 832 Sala S., Benini L., V., C., B., V.L., V., D.L., R., P., 2019. Suggestions for the update of the Environmental Footprint Life Cycle
833 Impact Assessment: Impacts due to resource use, water use, land use, and particulate matter. EUR 28636 EN,
834 Publications Office of the European Union, Luxembourg,. <https://doi.org/10.2760/78072>
- 835 Schmidinger, K., Stehfest, E., 2012. Including CO2 implications of land occupation in LCAs — method and example for
836 livestock products. *Int. J. Life Cycle Assess.* 17, 962–972. <https://doi.org/10.1007/s11367-012-0434-7>
- 837 SDES, 2019. Chiffres clés du climat – France, Europe et Monde. Le service de la donnée et des études statistiques (SDES)-
838 Ministère de la Transition Ecologique et Solidaire (MTES), Paris, France.
- 839 Shi, Z., Crowell, S., Luo, Y., Moore, B., 2018. Model structures amplify uncertainty in predicted soil carbon responses to
840 climate change. *Nat. Commun.* 9, 1–11. <https://doi.org/10.1038/s41467-018-04526-9>
- 841 Shibu, M.E., Leffelaar, P.A., Van Keulen, H., Aggarwal, P.K., 2006. Quantitative description of soil organic matter dynamics-

- 842 A review of approaches with reference to rice-based cropping systems. *Geoderma* 137, 1–18.
843 <https://doi.org/10.1016/j.geoderma.2006.08.008>
- 844 Smith, W.N., Grant, B.B., Campbell, C.A., McConkey, B.G., Desjardins, R.L., Kröbel, R., Malhi, S.S., 2012. Crop residue
845 removal effects on soil carbon: Measured and inter-model comparisons. *Agric. Ecosyst. Environ.* 161, 27–38.
846 <https://doi.org/10.1016/j.agee.2012.07.024>
- 847 Sommer, R., Bossio, D., 2014. Dynamics and climate change mitigation potential of soil organic carbon sequestration. *J.*
848 *Environ. Manage.* 144, 83–87. <https://doi.org/10.1016/j.jenvman.2014.05.017>
- 849 Strullu, L., Beaudoin, N., de Cortàzar Aauri, I.G., Mary, B., 2014. Simulation of Biomass and Nitrogen Dynamics in
850 Perennial Organs and Shoots of *Miscanthus* × *Giganteus* Using the STICS Model. *Bioenergy Res.* 7, 1253–1269.
851 <https://doi.org/10.1007/s12155-014-9462-4>
- 852 UNFCCC, 2018. Climate Get the Big Picture - A guide to the UNFCCC and its processes [WWW Document]. United Nations
853 Conv. Clim. Chang. URL <https://bigpicture.unfccc.int/> (accessed 1.1.18).
- 854 UNIFA, 1998. Chapter 1: Le Sol, in: *La Fertilisation*. UNIFA - Union des Industries de la Fertilisation (UNIFA), Union des
855 Industries de la Fertilisation., pp. 1–78.
- 856 White, R.E., Davidson, B., Lam, S.K., Chen, D., 2018. A critique of the paper ‘Soil carbon 4 per mille’ by Minasny et al.
857 (2017).’ *Geoderma* 309, 115–117. <https://doi.org/10.1016/j.geoderma.2017.05.025>
- 858 Wiesmeier, M., Hübner, R., Dechow, R., Maier, H., Spörlein, P., Geuß, U., Hangen, E., Reischl, A., Schilling, B., Lützow, M.
859 Von, Kögel-knabner, I., 2014. Estimation of past and recent carbon input by crops into agricultural soils of southeast
860 Germany. *Eur. J. Agron.* 61, 10–23. <https://doi.org/10.1016/j.eja.2014.08.001>
- 861 Wiesmeier, M., Urbanski, L., Hobley, E., Lang, B., Lützow, M. von, Marin-Spiotta, E., Wesemael, B. van, Rabot, E., Ließ, M.,
862 Garcia-Franco, N., Wollschläger, U., Vogel, H.-J., Kögel-Knabner, I., 2019. Soil organic carbon storage as a key
863 function of soils - A review of drivers and indicators at various scales. *Geoderma* 333, 149–162.
864 <https://doi.org/10.1016/j.geoderma.2018.07.026>
- 865 Zanella, A., Bolzonella, C., Lowenfels, J., Ponge, J.F., Bouché, M., Saha, D., Kukal, S.S., Fritz, I., Savory, A., Blouin, M., Sartori,
866 L., Tatti, D., Kellermann, L.A., Trachsel, P., Burgos, S., Minasny, B., Fukuoka, M., 2018. Humusica 2, article 19: Techno
867 humus systems and global change—conservation agriculture and 4/1000 proposal. *Appl. Soil Ecol.* 122, 271–296.
868 <https://doi.org/10.1016/j.apsoil.2017.10.036>
- 869 Zang, H., Blagodatskaya, E., Wen, Y., Xu, X., Dyckmans, J., Kuzyakov, Y., 2018. Carbon sequestration and turnover in soil
870 under the energy crop *Miscanthus*: repeated ^{13}C natural abundance approach and literature synthesis. *GCB*
871 *Bioenergy* 10, 262–271. <https://doi.org/10.1111/gcbb.12485>
- 872 Zhong, Z., Chen, Z., Xu, Y., Ren, C., Yang, G., Han, X., Ren, G., Feng, Y., 2018. Relationship between Soil Organic Carbon
873 Stocks and Clay Content under Different Climatic Conditions in Central China. *Forests* 9, 598.
874 <https://doi.org/10.3390/f9100598>
- 875 Zomer, R.J., Bossio, D.A., Sommer, R., Verchot, L. V., 2017. Global Sequestration Potential of Increased Organic Carbon in
876 Cropland Soils. *Sci. Rep.* 7, 1–8. <https://doi.org/10.1038/s41598-017-15794-8>
- 877

878 **Figure captions**

879 Fig. 1. Coupling diagram of energy system and soil organic carbon modelling for dynamic carbon accounting
880 (Acronyms: A: Age, C: Carbon content, DBH: Diameter Breast Height, H: Height, H: Humification coefficient, K:
881 Mineralisation coefficient, NPP: Net Primary Productivity, SOC: Soil Organic Carbon, V: Volume)

882 Fig. 2. Policy scenario simulations (BAU, 15BIO, LTECV) linked with first (1G) and second (2G) generation
883 bioethanol and biodiesel pathways in terms of a) land use requirements in ha, b) biomass commodity supply in
884 kt, c) equivalent energy supply in MJ, and d) associated Greenhouse Gas emissions in kt CO₂-eq

885 Fig. 3. Soil carbon inputs per biomass commodity from above- and belowground plant compartments, including
886 exogenous matter. Pie chart represents the average proportions

887 Fig. 4. Soil organic carbon inventories over a time horizon of 100 years [kt CO₂] per TIMES-MIRET (BAU, 15BIO,
888 LTECV) and C input (S2_AG, S3_BG, S4_EX) scenarios

889 Fig. 5. Instantaneous [W·m⁻²] and cumulative [W·yr·m⁻²] radiative forcing per policy (BAU, 15BIO and LTECV)
890 and C input (S1_TOT, S2_AG, S3_BG, S4_EX) scenarios, denoting the dynamic impacts from biogenic- (here SOC
891 flows) and fossil- (C neutral) sourced emissions, as well the sum of both in C-complete

892 Fig. 6. Cumulative radiative forcing [W·yr·m⁻²] per policy (BAU, 15BIO and LTECV) and C input (S2_AG, S3_BG,
893 S4_EX) scenarios

894 Fig. 7. Cumulative radiative forcing [W·yr·m⁻²] from the sensitivity analysis results a) over the time horizon 2019
895 to 2119, b) quantitative uncertainty concerning k coefficient and temperature variations, and c) effect from
896 changes in C inputs. b) and c) represent the year 2019 including uncertainty (error bar represent the minimum
897 attainable value)

898

Modelling dynamic soil organic carbon flows of annual and perennial energy crops to inform energy-transport policy scenarios in France

Ariane Albers^{a, b, c, *}, Angel Avadí^{c, d, f}, Anthony Benoist^{c, e, f}, Pierre Collet^a, Arnaud Hélias^{b, g, h}

^a IFP Energies Nouvelles, 1 et 4 Avenue de Bois-Préau, 92852 Rueil-Malmaison, France

^b LBE, Montpellier SupAgro, INRA, UNIV Montpellier, Narbonne, France

^c Elsa, Research Group for Environmental Lifecycle and Sustainability Assessment, Montpellier, France

^d CIRAD, UPR Recyclage et risque, F-34398 Montpellier, France

^e CIRAD, UPR BioWooEB, F-34398 Montpellier, France

^f Univ Montpellier, CIRAD, Montpellier, France

^g Chair of Sustainable Engineering, Technische Universität Berlin, Berlin, Germany

^h ITAP, Irstea, Montpellier SupAgro, Univ Montpellier, ELSA Research Group, Montpellier, France

* Corresponding author: ariane.albers@ifpen.fr

Tables

Table 1. Comparison of recommended static modelling approaches for calculating soil quality SOM/SOC changes associated with LU (occupation) and LUC (transformation) in LCA

Method	Recommending guideline	Land activities included	Usefulness for LCIA	Notes
SOM/SOC change (Brandão and Milà i Canals, 2013; Milà i Canals et al., 2007a, 2007b)	International Reference Life Cycle Data System (EC-JRC, 2010)	T+O	CF available, limited linking to AoP	Informing soil quality, site-dependent or -generic, but not climate change
LANCA (Beck et al., 2010; Bos et al., 2016; Horn and Maier, 2018)	Product Environmental Footprint Category Rules (EC, 2018b)	T+O	CF available	Informing soil functions, data intensive, suitable for site- dependent or generic assessment
SALCA-SQ (Oberholzer et al., 2012, 2006)	ecoinvent v2 (Nemecek et al., 2011; Nemecek and Kagi, 2007)	O	CF available, limited linking to AoP	Informing soil properties and treats, site-dependent or site-specific (plot level)
Müller-Wenk and Brandão (2010)	UNEP-SETAC (Koellner et al., 2013)	T+O	CF available	Informing climate change, site-generic (6 biomes over the world)
PAS 2050 standard (BSI, 2011) and IPCC Guideline for National GHG Inventories (IPCC, 2006)	Product Environmental Footprint Category Rules (EC, 2018b)	T	N/A	Dynamic modelling in the context of CDM methodologies, but site-dependent

Acronyms. AoP: Area of Protection, SOC: Soil Organic Carbon, SOM: Soil Organic Matter, T: Transformation; O: Occupation, LCIA: Life Cycle Impact Assessment, CF: characterisation factors, GHG: Greenhouse Gas, CDM: Kyoto Protocol's Clean Development Mechanism

Sources: Benoist and Bessou (2018)

Table 2. Isohumic coefficient (h), carbon (C) content, carbon partitioning from net primary productivity (NPP), and mean French agricultural practices regarding fertilisation of energy crops and exogenous inputs

Crops and residues	Yields [t·ha ⁻¹]	Isohumic coefficient (h) [unitless]	C content [t·t ⁻¹]	Carbon partitioning per plant fraction (calculated)				NPP [t C·ha ⁻¹]	Fertilisation of cultivation of energy crops (calculated)									
				C _P [t C·ha ⁻¹]	C _S [t C·ha ⁻¹]	C _R [t C·ha ⁻¹]	C _E [t C·ha ⁻¹]		Mineral N [kg·ha ⁻¹]	Cattle effluents [t·ha ⁻¹]	Poultry effluents [t·ha ⁻¹]	Swine effluents [t·ha ⁻¹]	Compost [t·ha ⁻¹]					
Maize	11.980	a	0.193	e	0.414	i	4.957	5.369	2.959	1.967	15.251	l	133	11.069	0.519	1.513	1.410	m
Rapeseed	3.655	a	0.244	f	0.502	i	1.901	10.231	3.393	2.238	17.763	l	169	3.989	0.187	0.545	0.508	m
Wheat	6.408	a	0.193	f	0.475	i	3.046	4.354	1.697	1.124	10.220	l	169	0.819	0.038	0.112	0.125	m
Triticale	5.501	a	0.125	e	0.475	i	2.615	5.088	1.428	0.925	10.056	l	107	5.265	0.247	0.720	0.671	m
Sunflower	2.720	b	0.200	e	0.440	i	1.197	1.795	0.330	0.000	3.322	l	123	2.843	0.133	0.389	0.362	m
Sugar beet	9.540	b	0.126	e	0.467	i	4.459	0.245	0.245	0.164	5.114	l	56	9.516	0.446	1.301	1.212	m
Soybean	3.479	c	0.230	g	0.440	j	1.531	2.291	0.735	0.478	5.035	l	8	0.000	0.000	0.000	0.000	m
Miscanthus	22.788	d	0.126	f	0.475	j	10.835	12.218	12.995	4.332	40.379	l	52	1.505	0.071	0.206	0.192	m
Switchgrass	15.714	a	0.126	e	0.497	k	7.805	0.000	5.451	3.54	16.796	l	65	0.983	0.046	0.134	0.125	m
Cattle effluents	N/A		0.558	h	0.055	k	N/A	N/A	N/A	N/A	N/A		N/A	N/A	N/A	N/A	N/A	
Poultry effluents	N/A		0.308	h	0.154	k	N/A	N/A	N/A	N/A	N/A		N/A	N/A	N/A	N/A	N/A	
Swine effluents	N/A		0.462	h	0.083	k	N/A	N/A	N/A	N/A	N/A		N/A	N/A	N/A	N/A	N/A	
Other soil amendments (proxy compost)	N/A		0.670	h	0.130	k	N/A	N/A	N/A	N/A	N/A		N/A	N/A	N/A	N/A	N/A	

Sources: a (AGRESTE, 2019), b (Besnard et al., 2014), c (Cattelan and Dall’Agnol, 2018), d (Strullu et al., 2014), e (Duparque et al., 2013; Irizar et al., 2015; Moreno et al., 2016; Saffih-Hdadi and Mary, 2008), f (UNIFA, 1998), g (Irizar et al., 2015; Moreno et al., 2016), h (Agro-Transfert, 2019; Bouthier et al., 2014), i (PHYLLIS 2 database, 2019), j (Ma et al., 2018), k (Avadí, 2019), l (Bolinder et al., 2007; Carvalho et al., 2017; Richter et al., 2016; Strullu et al., 2014), for miscanthus aboveground inputs between 40% and 67% (Carvalho et al., 2017; Strullu et al., 2014) and perennial belowground proportions of rhizomes 75% and roots 25% (Agostini et al., 2015), m (AGRESTE, 2019, 2014, 2011; Avadí, 2019; FAO, 2004). “Effluents” refers to average values from manures, slurries and droppings (poultry). Modelling details of specific crops: maize (as a mean of grain and fodder), miscanthus (as permanent prairie), switchgrass (as temporary prairie), and wheat (as a mean of hard and soft).

Descriptions of sub-indices: P - agricultural aboveground product, S - residual aboveground compartment, R - root/rhizome tissue, E - extra-root material.

Modelling dynamic soil organic carbon flows of annual and perennial energy crops to inform energy-transport policy scenarios in France

Ariane Albers^{a, b, c, *}, Angel Avadí^{c, d, f}, Anthony Benoist^{c, e, f}, Pierre Collet^a, Arnaud Hélias^{b, g, h}

^a IFP Energies Nouvelles, 1 et 4 Avenue de Bois-Préau, 92852 Rueil-Malmaison, France

^b LBE, Montpellier SupAgro, INRA, UNIV Montpellier, Narbonne, France

^c Elsa, Research Group for Environmental Lifecycle and Sustainability Assessment, Montpellier, France

^d CIRAD, UPR Recyclage et risque, F-34398 Montpellier, France

^e CIRAD, UPR BioWooEB, F-34398 Montpellier, France

^f Univ Montpellier, CIRAD, Montpellier, France

^g Chair of Sustainable Engineering, Technische Universität Berlin, Berlin, Germany

^h ITAP, Irstea, Montpellier SupAgro, Univ Montpellier, ELSA Research Group, Montpellier, France

* Corresponding author: ariane.albers@ifpen.fr

Figures

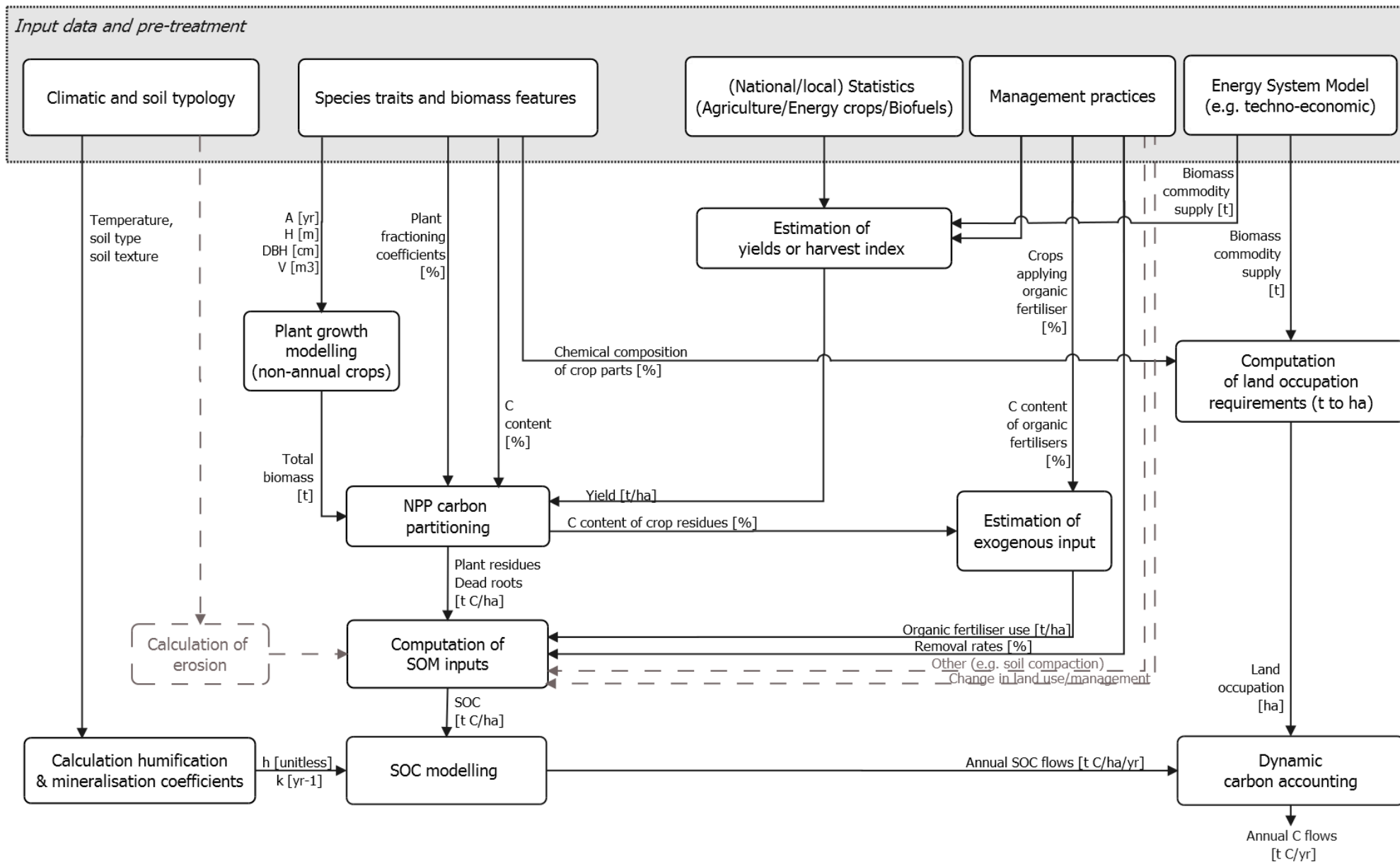


Fig. 1. Coupling diagram of energy system and soil organic carbon modelling for dynamic carbon accounting (Acronyms: A: Age, C: Carbon content, DBH: Diameter Breast Height, H: Height, h: Humification coefficient, k: Mineralisation coefficient, NPP: Net Primary Productivity, SOC: Soil Organic Carbon, V: Volume)

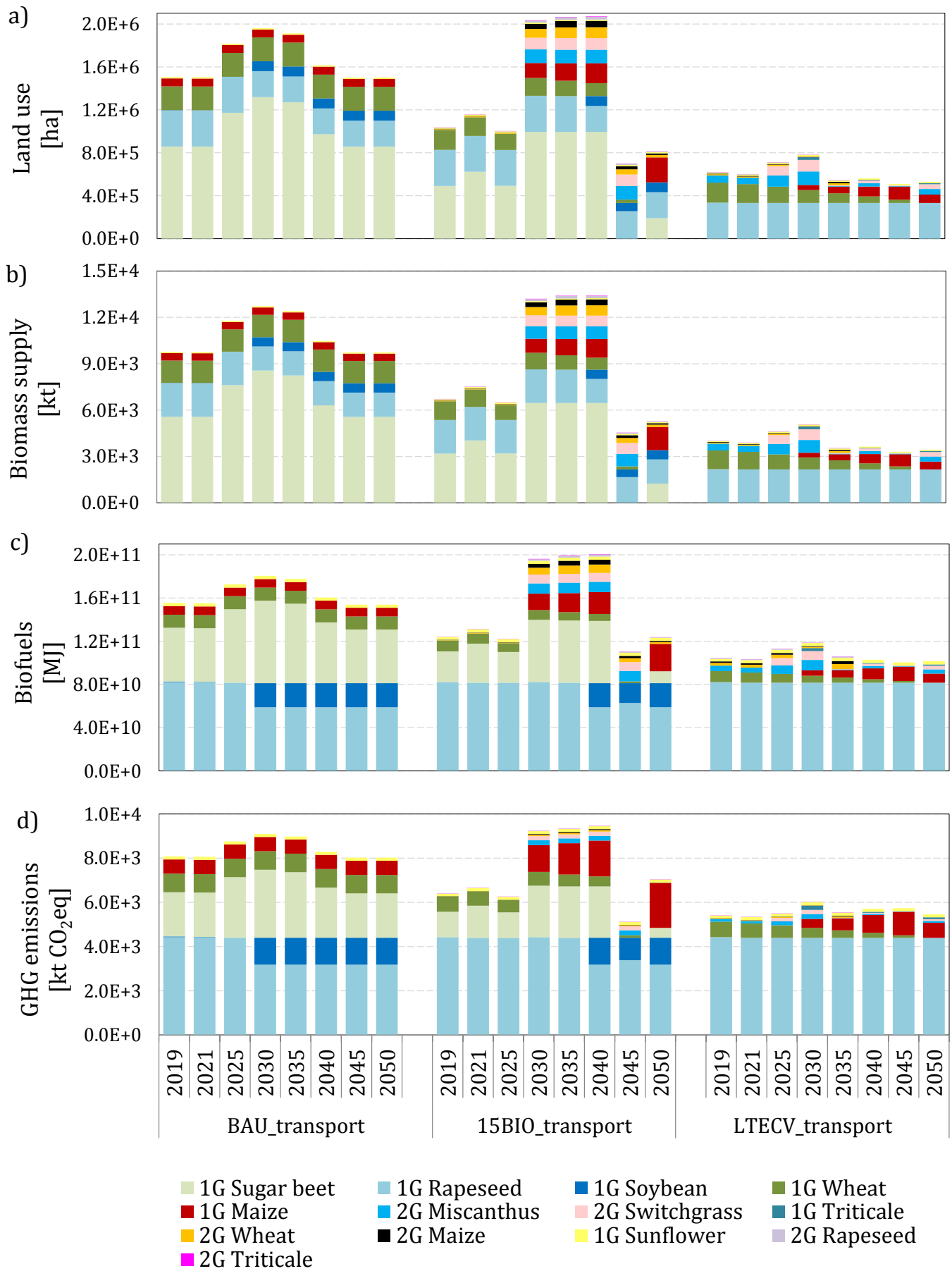


Fig. 2. Policy scenario simulations (BAU, 15BIO, LTECV) linked with first (1G) and second (2G) generation bioethanol and biodiesel pathways in terms of a) land use requirements in ha, b) biomass commodity supply in kt, c) equivalent energy supply in MJ, and d) associated Greenhouse Gas emissions in kt CO₂-eq

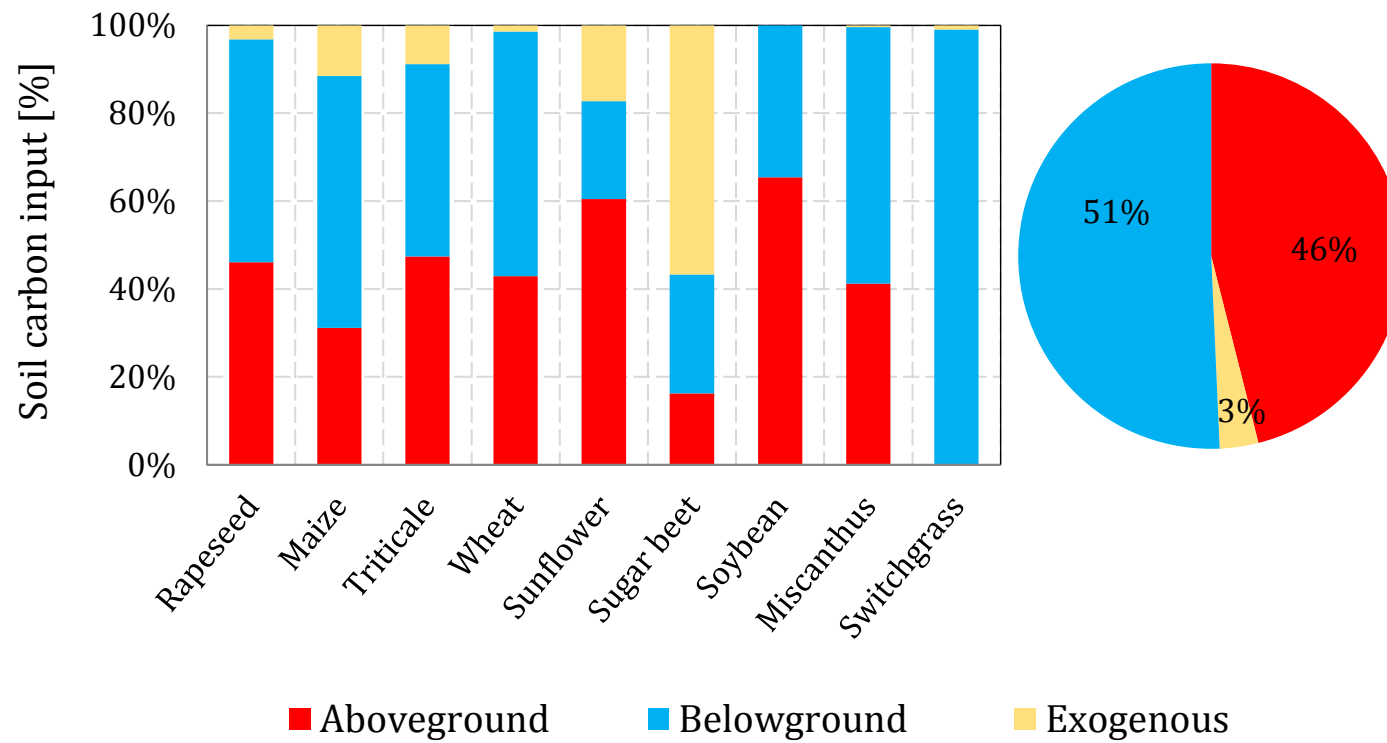


Fig. 3. Soil carbon inputs per biomass commodity from above- and belowground plant compartments, including exogenous matter. Pie chart represents the average proportions

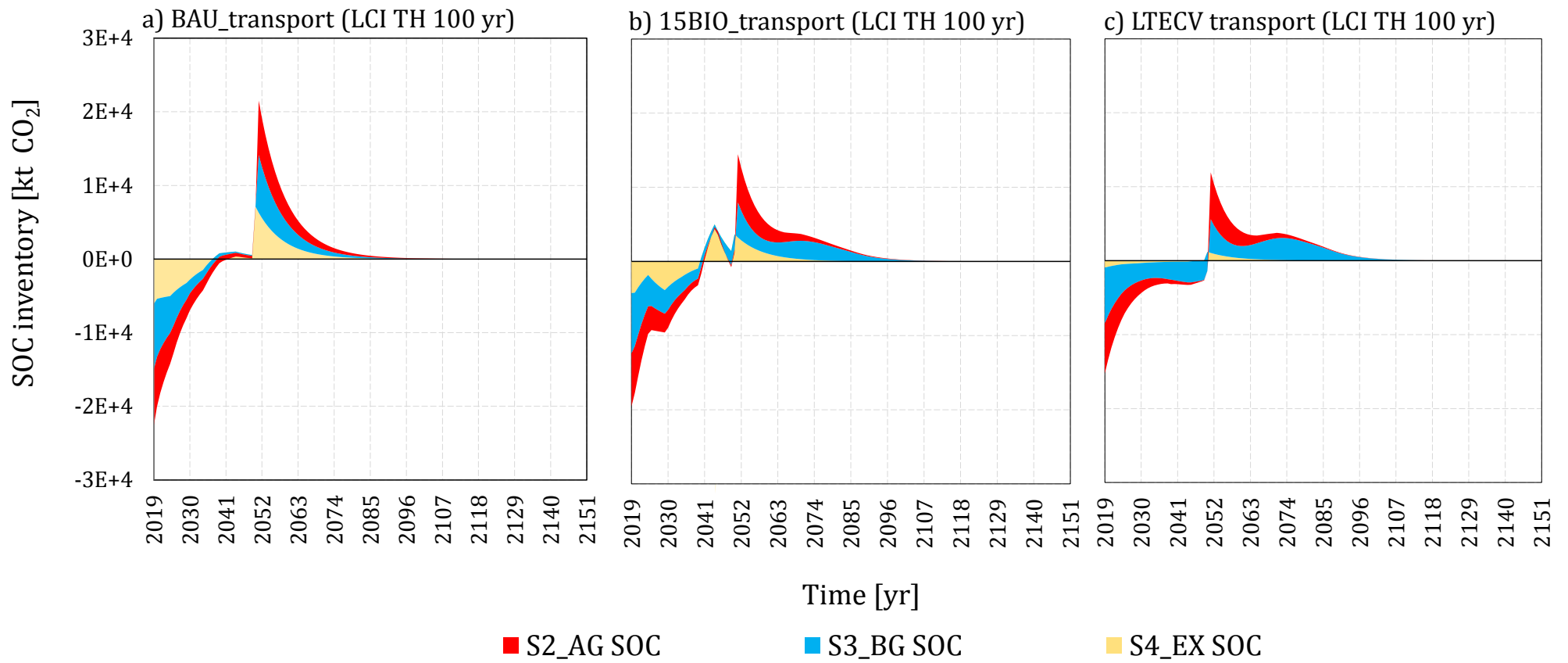


Fig. 4. Soil organic carbon inventories over a time horizon of 100 years [kt CO₂] per TIMES-MIRET (BAU, 15BIO, LTECV) and C input (S2_AG, S3_BG, S4_EX) scenarios

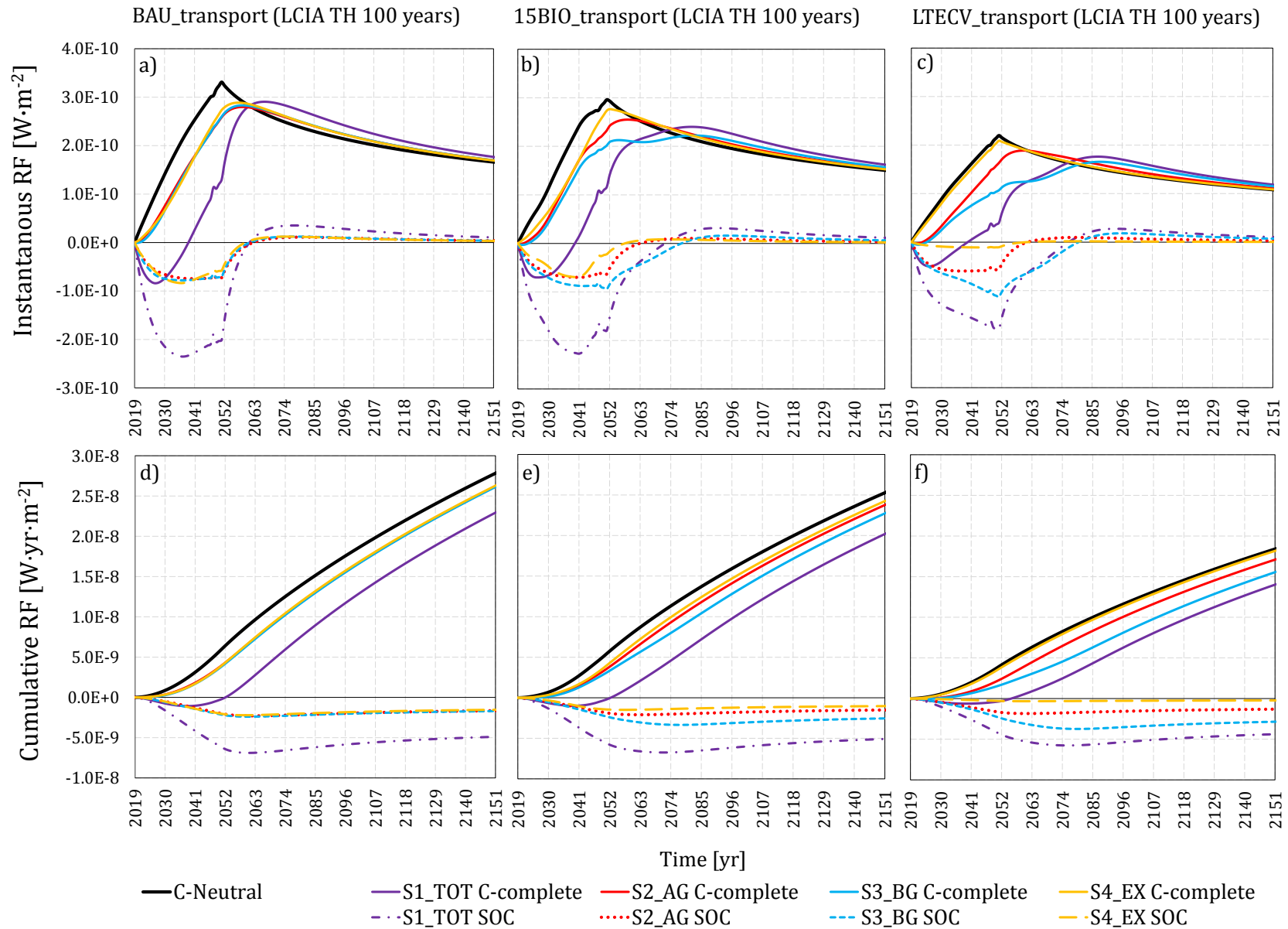


Fig. 5. Instantaneous [W·m⁻²] and cumulative [W·yr·m⁻²] radiative forcing per policy (BAU, 15BIO and LTECV) and C input (S1_TOT, S2_AG, S3_BG, S4_EX) scenarios, denoting the dynamic impacts from biogenic- (here SOC flows) and fossil- (C neutral) sourced emissions, as well the sum of both in C-complete

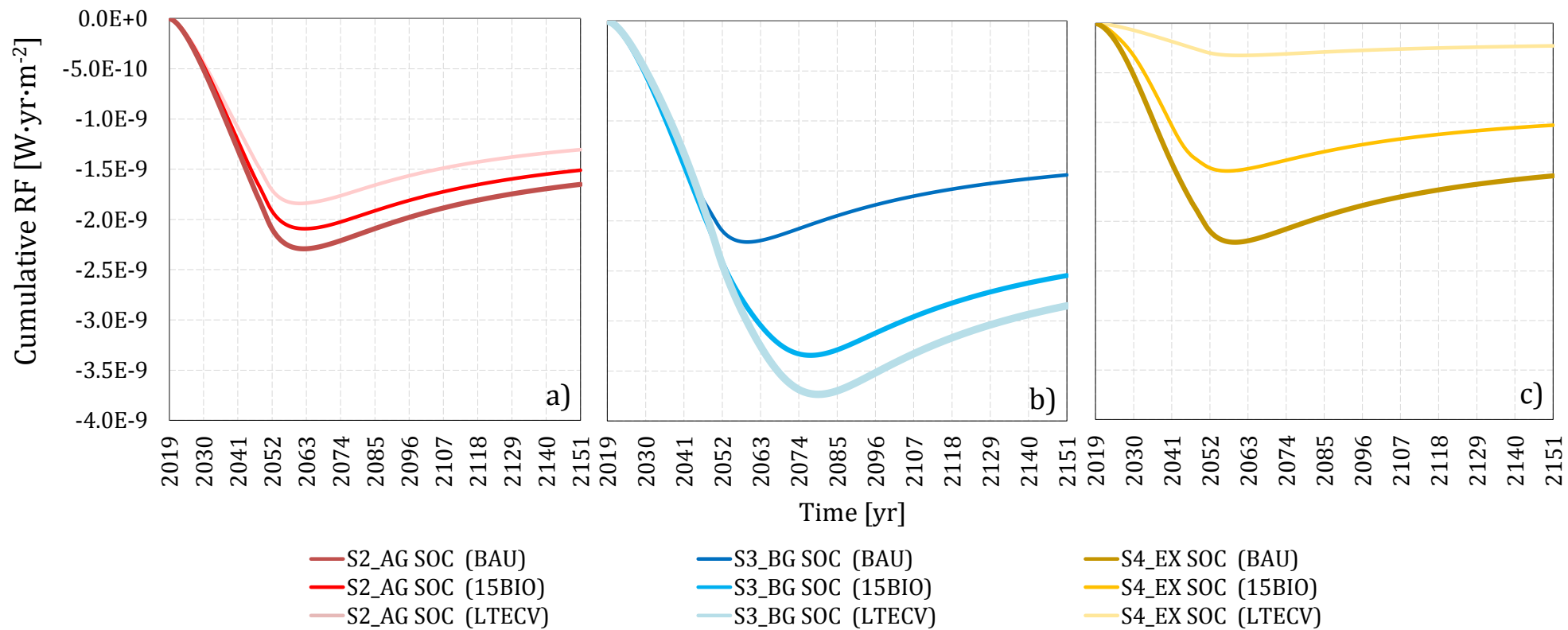


Fig. 6. Cumulative radiative forcing [W·yr·m⁻²] per policy (BAU, 15BIO and LTECV) and C input (S2_AG, S3_BG, S4_EX) scenarios

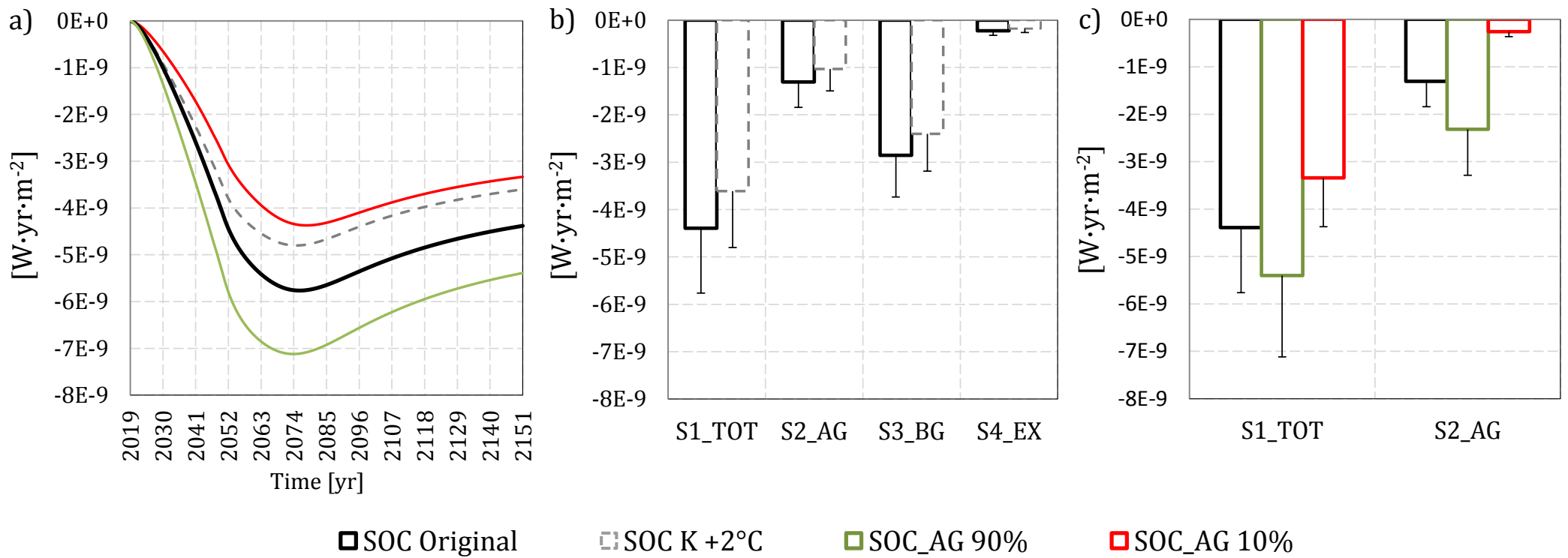


Fig. 7. Cumulative radiative forcing [W·yr·m⁻²] from the sensitivity analysis results a) over the time horizon 2019 to 2119, b) quantitative uncertainty concerning k coefficient and temperature variations, and c) effect from changes in C inputs. b) and c) represent the year 2019 including uncertainty (error bar represent the minimum attainable value)

Supplementary material for on-line publication only

[Click here to download Supplementary material for on-line publication only: Supplementary Material.pdf](#)